

Donald E. Marshall[†] and Steffen Rohde[†]

Department of Mathematics

University of Washington

Abstract

In the early 1980's an elementary algorithm for computing conformal maps was discovered by R. Kühnau and the first author. The algorithm is fast and accurate, but convergence was not known. Given points z_0, \dots, z_n in the plane, the algorithm computes an explicit conformal map of the unit disk onto a region bounded by a Jordan curve γ with $z_0, \dots, z_n \in \gamma$. We prove convergence for Jordan regions in the sense of uniformly close boundaries, and give corresponding uniform estimates on the closed region and the closed disc for the mapping functions and their inverses. Improved estimates are obtained if the data points lie on a C^1 curve or a K -quasicircle. The algorithm was discovered as an approximate method for conformal welding, however it can also be viewed as a discretization of the Löwner differential equation.

§0. Introduction

Conformal maps have useful applications to problems in physics, engineering and mathematics, but how do you find a conformal map say of the upper half plane \mathbb{H} to a complicated region? Rather few maps can be given explicitly by hand, so that a computer must be used to find the map approximately. One reasonable way to describe a region numerically is to give a large number of points on the boundary. One way to say that a computed map defined on \mathbb{H} is “close” to a map to the region is to require that the boundary of the image be uniformly close to the polygonal curve through the data points. Indeed, the only information we may have about the boundary of a region are these data points.

[†]The authors are supported in part by NSF grants DMS-0201435 and DMS-0244408.

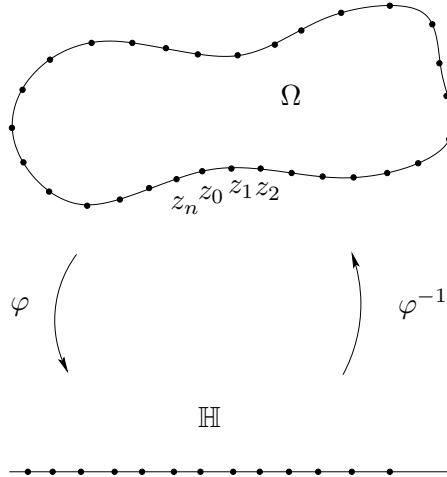


Figure 1.

In the early 1980's an elementary algorithm was discovered independently by R. Kühnau [K] and the first author. The algorithm is fast and accurate, but convergence was not known. The purpose of this paper is to prove convergence in the sense of uniformly close boundaries, and discuss related numerical issues. One important aspect of the algorithm that sets it apart from others: in many applications both the conformal map and its inverse are required; this algorithm finds both simultaneously.

The algorithm can be viewed as a discretization of the Loewner differential equation, or as an approximate solution to a conformal welding problem. The approximation to the conformal map is obtained as a composition of conformal maps onto slit halfplanes. Depending on the type of slit (hyperbolic geodesic, straight line segment or circular arc) we actually obtain different versions of this algorithm. These are described in Section 1.

We then focus our attention on the “geodesic algorithm” and study its behaviour in different situations. The easiest case is discussed in Section 2: If the data points z_0, z_1, \dots are the consecutive contact points of a chain of disjoint discs (see Figures 7 and 8 below), then a simple but very useful reinterpretation of the algorithm, together with the hyperbolic convexity of discs in simply connected domains (Jørgensen's theorem), implies that the curve produced by the algorithm is confined to the chain of discs (Theorem 2.2). One consequence is that for any bounded simply connected domain Ω , the geodesic algorithm can be used to compute a conformal map to a Jordan region Ω_c (“c” for computed) so that the Hausdorff distance between $\partial\Omega$ and $\partial\Omega_c$ is as small as desired (Theorem 2.4).

In Section 3, we describe an extension of the ideas of Section 2 that applies to a variety of domains such as smooth domains or quasiconformal discs with small constants, with better estimates. For instance, if $\partial\Omega$ is a C^1 curve, then the geodesic algorithm can be used to compute a conformal map to a Jordan region Ω_c with $\partial\Omega_c \in C^1$ so that the boundaries are uniformly close and so that the unit tangent vectors are uniformly close (Theorem 3.10). The heart of the convergence proof in these cases is the technical “self-improvement” Lemmas 3.5 and 3.6. In fact, this approach constituted our first convergence proof.

The basic conformal maps and their inverses used in the geodesic algorithm are given in terms of linear fractional transformations, squares and square roots. The slit and zipper algorithms use elementary maps whose inverses cannot be written in terms of elementary maps. Newton’s method, however, converges so rapidly that it provides virtually a formula for the inverses. In Section 4 we discuss how to apply variants of Newton’s method by dividing the plane into four regions, and prove quadratic convergence in one region. We plan to address the convergence of the slit and zipper variants of the algorithm in a forthcoming paper.

In Sections 5 and 6, we show how estimates on the distance between boundaries of Jordan regions gives estimates on the uniform distance between the corresponding conformal maps to \mathbb{D} , and apply these estimates to obtain bounds for the convergence of the conformal maps produced by the algorithm. We summarize some of our results as follows: If $\partial\Omega$ is contained in a chain of discs of radius $\leq \epsilon$ with the data points being the contact points of the discs, or if $\partial\Omega$ is a K -quasicircle with K close to one and if the data points are consecutive points on $\partial\Omega$ of distance comparable to ϵ , then the Hausdorff distance between $\partial\Omega$ and the boundary of the domain computed by the geodesic algorithm, $\partial\Omega_c$, is at most ϵ and the conformal maps φ, φ_c onto \mathbb{D} satisfy

$$\sup_{\Omega \cap \Omega_c} |\varphi - \varphi_c| \leq C\epsilon^p,$$

where any $p < 1/2$ works in the disc-chain case, and p is close to 1 if K is close to one. In the case of quasicircles, we also have

$$\sup_{\mathbb{D}} |\varphi^{-1} - \varphi_c^{-1}| \leq C\epsilon^p$$

with p close to one. Better estimates are obtained for regions bounded by smoother Jordan curves.

Section 7 contains a brief discussion of numerical results. The Appendix has a simple self-contained proof of Jørgensen’s theorem.

The first author would like to express his deep gratitude to L. Carleson for our exciting investigations at Mittag-Leffler Institute 1882-83 which led to the discovery of the zipper algorithms.

§1. Conformal mapping algorithms

The Geodesic Algorithm

The most elementary version of the conformal mapping algorithm is based on the simple map $f_a : \mathbb{H} \setminus \gamma \rightarrow \mathbb{H}$ where γ is an arc of a circle from 0 to $a \in \mathbb{H}$ which is orthogonal to \mathbb{R} at 0. This map can be realized by a composition of a linear fractional transformation, the square and the square root map as illustrated in Figure 2. The orthogonal circle also meets \mathbb{R} orthogonally at a point $b = |a|^2/\text{Re}a$ and is illustrated by a dashed curve in Figure 2.

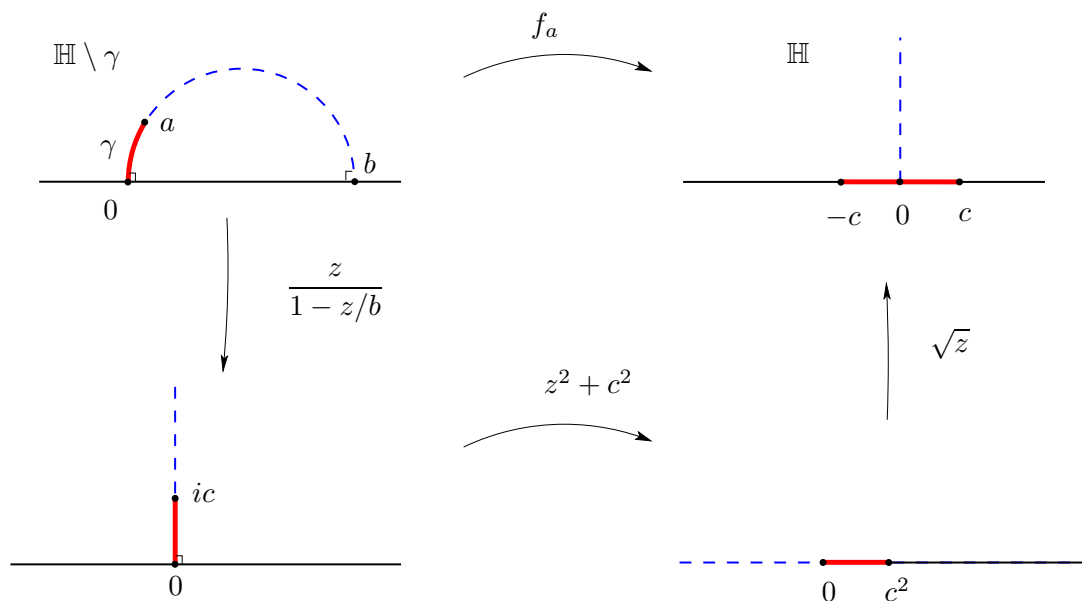


Figure 2. The basic map f_a .

In Figure 2, $c = |a|^2/\text{Im}a$. Observe that the arc γ is opened to two adjacent intervals at 0 with a , the tip of γ , mapped to 0. The inverse f_a^{-1} can be easily found by composing the inverses of these elementary maps in the reverse order.

Now suppose that z_0, z_1, \dots, z_n are points in the plane. The basic maps f_a can be used to compute a conformal map of \mathbb{H} onto a region Ω_c bounded by a Jordan curve which passes through the data points as illustrated in Figure 3.

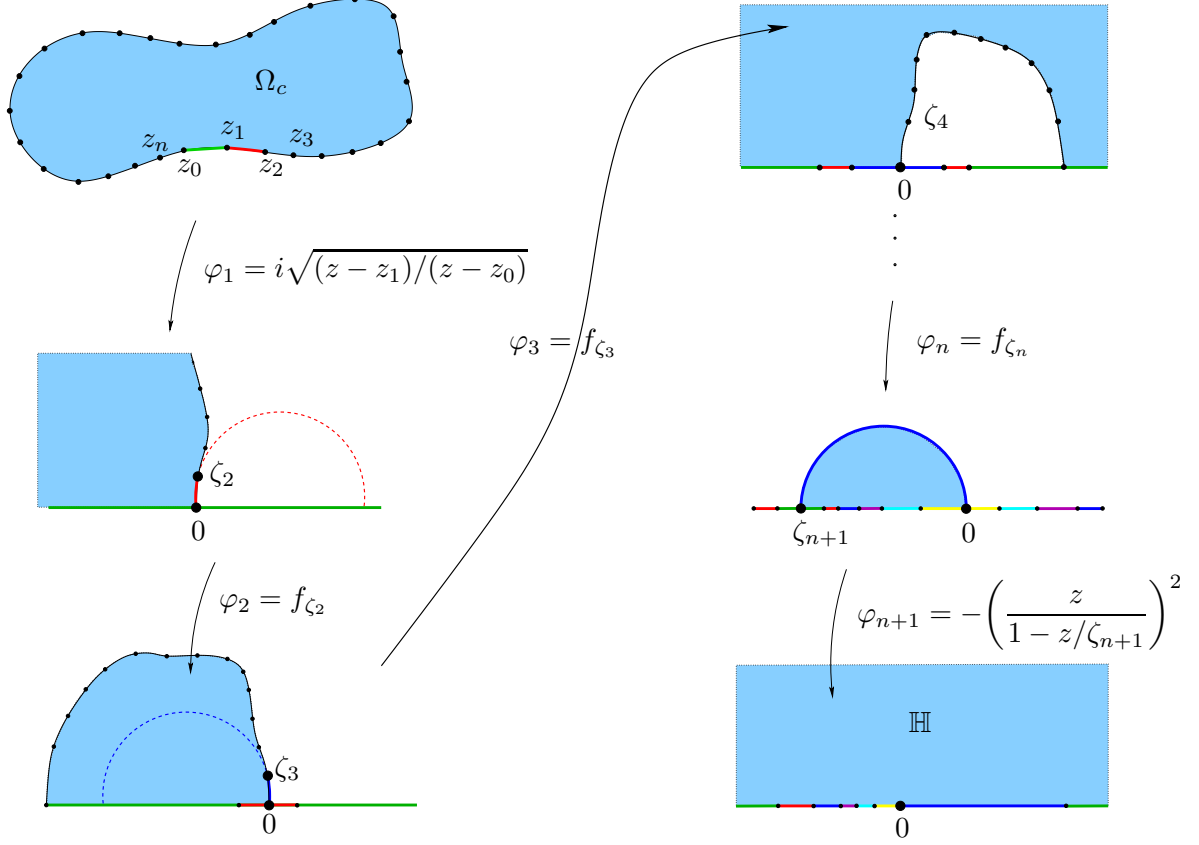


Figure 3. The Geodesic Algorithm.

The complement in the extended plane of the line segment from z_0 to z_1 can be mapped onto \mathbb{H} with the map

$$\varphi_1(z) = i\sqrt{\frac{z-z_1}{z-z_0}}$$

and $\varphi_1(z_1) = 0$ and $\varphi_1(z_0) = \infty$. Set $\zeta_2 = \varphi_1(z_2)$ and $\varphi_2 = f_{\zeta_2}$. Repeating this process, define

$$\zeta_k = \varphi_{k-1} \circ \varphi_{k-2} \circ \dots \circ \varphi_1(z_k)$$

and

$$\varphi_k = f_{\zeta_k}.$$

for $k = 2, \dots, n$. Finally, map a half-disc to \mathbb{H} by letting

$$\zeta_{n+1} = \varphi_n \circ \dots \circ \varphi_1(z_0) \in \mathbb{R}$$

be the image of z_0 and set

$$\varphi_{n+1} = \pm \left(\frac{z}{1-z/\zeta_{n+1}} \right)^2$$

The + sign is chosen in the definition of φ_{n+1} if the data points have negative winding number (clockwise) around an interior point of $\partial\Omega$, and otherwise the – sign is chosen. Set

$$\varphi = \varphi_{n+1} \circ \varphi_n \circ \dots \circ \varphi_2 \circ \varphi_1$$

and

$$\varphi^{-1} = \varphi_1^{-1} \circ \varphi_2^{-1} \circ \dots \circ \varphi_{n+1}^{-1}.$$

Then φ^{-1} is a conformal map of \mathbb{H} onto a region Ω_c such that $z_j \in \partial\Omega_c$, $j = 0, \dots, n$. The portion γ_j of $\partial\Omega_c$ between z_j and z_{j+1} is the image of the arc of a circle in the upper half plane by the analytic map $\varphi_1^{-1} \circ \dots \circ \varphi_j^{-1}$. In more picturesque language, after applying φ_1 , we grab the ends of the displayed horizontal line segment and pull, splitting apart or unzipping the curve at 0. The remaining data points move down until they hit 0 and then each splits into two points, one on each side of 0, moving further apart as we continue to pull.

As an aside, we make a few comments. As mentioned $\partial\Omega_c$ is piecewise analytic. It is easy to see that it is also C^1 since the inverse of the basic map f_a in Figure 2 doubles angles at 0 and halves angles at $\pm c$. In fact it is also $C^{\frac{3}{2}}$ (see Proposition 3.12). If the data points $\{z_j\}$ lie on the boundary of a given region $\partial\Omega$, the analyticity of $\partial\Omega_c$ also allows us in many situations (see Proposition 2.5 and Corollary 3.9) to extend φ_c analytically across $\partial\Omega_c$ so that the extended map is a conformal map of Ω onto a region with boundary very close to $\partial\mathbb{D}$. Note also that φ is a conformal map of the complement of Ω_c , $\mathbb{C}^* \setminus \overline{\Omega_c}$, onto the lower half plane, $\mathbb{C} \setminus \overline{\mathbb{H}}$ where \mathbb{C}^* denotes the extended plane. Simply follow the unshaded region in \mathbb{H} in Figure 3. Finally, we remark that it is easier to use geodesic arcs in the right-half plane instead of in the upper-half plane when coding the algorithm, because most computer languages adopt the convention $-\frac{\pi}{2} < \arg \sqrt{z} \leq \frac{\pi}{2}$.

The Slit Algorithm

Given a region Ω , then we can select boundary points z_0, \dots, z_n on $\partial\Omega$ and apply the geodesic algorithm. We can view the circular arcs γ for the basic maps f_a as approximating the image of the boundary of Ω between 0 and a with a circular arc at each stage. We can improve the approximation by using straight lines instead of orthogonal arcs. So in the slit algorithm we replace the inverse of the maps f_a by conformal maps $g_a : \mathbb{H} \rightarrow \mathbb{H} \setminus L$ where L is a line segment from 0 to a . Explicitly

$$g_a(z) = C(z-p)^p(z+1-p)^{1-p}$$

where $p = \arg a/\pi$ and $C = |a|/p^p(1-p)^{1-p}$.

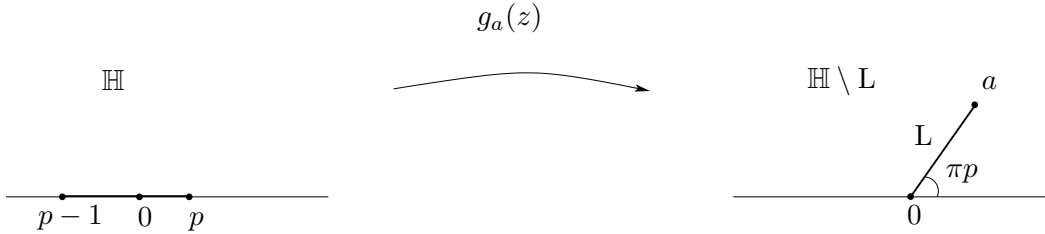


Figure 4. The Slit Maps.

One way to see that g_a is a conformal map, is to note that as x traces the real line from $-\infty$ to $+\infty$, $g_a(x)$ traces the boundary of $\mathbb{H} \setminus L$ and $g_a(z) \sim Cz$ for large z and then apply the argument principle. Another method would be to construct $Re \log g_a$ using harmonic measure as in the first two pages of [GM]. As in the basic maps of the geodesic algorithm, the line segment from 0 to a is opened to two adjacent intervals on \mathbb{R} by $f_a = g_a^{-1}$ with $f_a(a) = 0$ and $f_a(\infty) = \infty$. The map f_a cannot be written in terms of elementary functions, but an effective and rapid numerical inverse will be described in section 4.

We note that as in the geodesic algorithm, the boundary of the region Ω_c computed with the slit algorithm will be piecewise analytic. However it will not be C^1 . A curve is called C^1 if the arc length parameterization has a continuous first derivative. In other words, the direction of the unit tangent vector is continuous. Indeed if g_a is the map illustrated by Figure 4, and if g_b is another such map then $g_b \circ g_a$ forms a curve with angles $2\pi p$ and $2\pi(1-p)$ on either side of the curve at $b = g_b(0)$. Since analytic maps preserve angles, the boundary of the computed region consists of analytic arcs with endpoints at the data points, and angles determined by the basic maps. This will allow us to accurately compute conformal maps to regions with (a finite number of) “corners”, or “bends”.

The Zipper Algorithm

We can further improve the approximation by replacing the linear slits with arcs of (non-orthogonal) circles. In this version we assume there are an even number of boundary points, $z_0, z_1, \dots, z_{2n+1}$. The first map is replaced by

$$\varphi_1(z) = \sqrt{\frac{(z - z_2)(z_1 - z_0)}{(z - z_0)(z_1 - z_2)}}$$

which maps the complement in the extended plane of the circular arc through z_0, z_1, z_2 onto \mathbb{H} . At each subsequent stage, instead of pulling down one point ζ_k , we can find a unique circular arc

through 0 and the (images of) the next two data points ζ_{2k-1} and ζ_{2k} . By a linear fractional transformation ℓ_a which preserves \mathbb{H} , this arc is mapped to a line segment (assuming the arc is not tangent to \mathbb{R} at 0. See Figure 5.

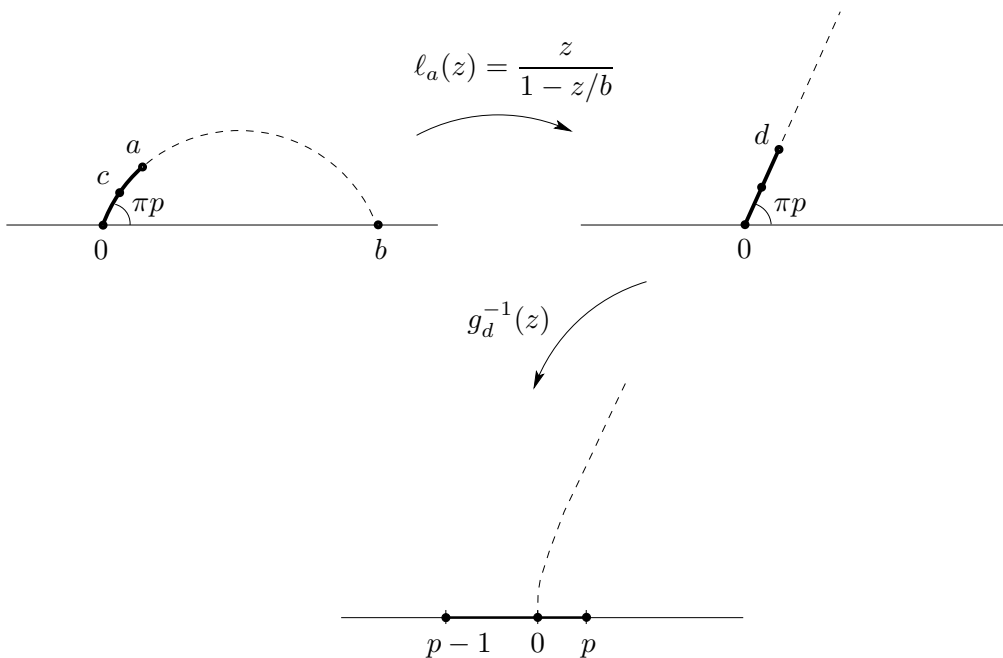


Figure 5. The Circular Slit Maps.

The complement of this segment in \mathbb{H} can then be mapped to \mathbb{H} as described in the slit algorithm, using g_d^{-1} where $d = a/(1 - a/b)$. The composition $h_{a,c} = g_d^{-1} \circ \ell_a$ then maps the complement of the circular arc in \mathbb{H} onto \mathbb{H} . Thus at each stage we are giving a “quadratic approximation” instead of a linear approximation to the (image of) the boundary. The last map φ_{n+1} is a conformal map of the intersection of a disc with \mathbb{H} where the boundary circular arc passes through 0, the image of z_{2n+1} and the image of z_0 by the composition $\varphi_n \circ \dots \circ \varphi_1$. See Figure 6.

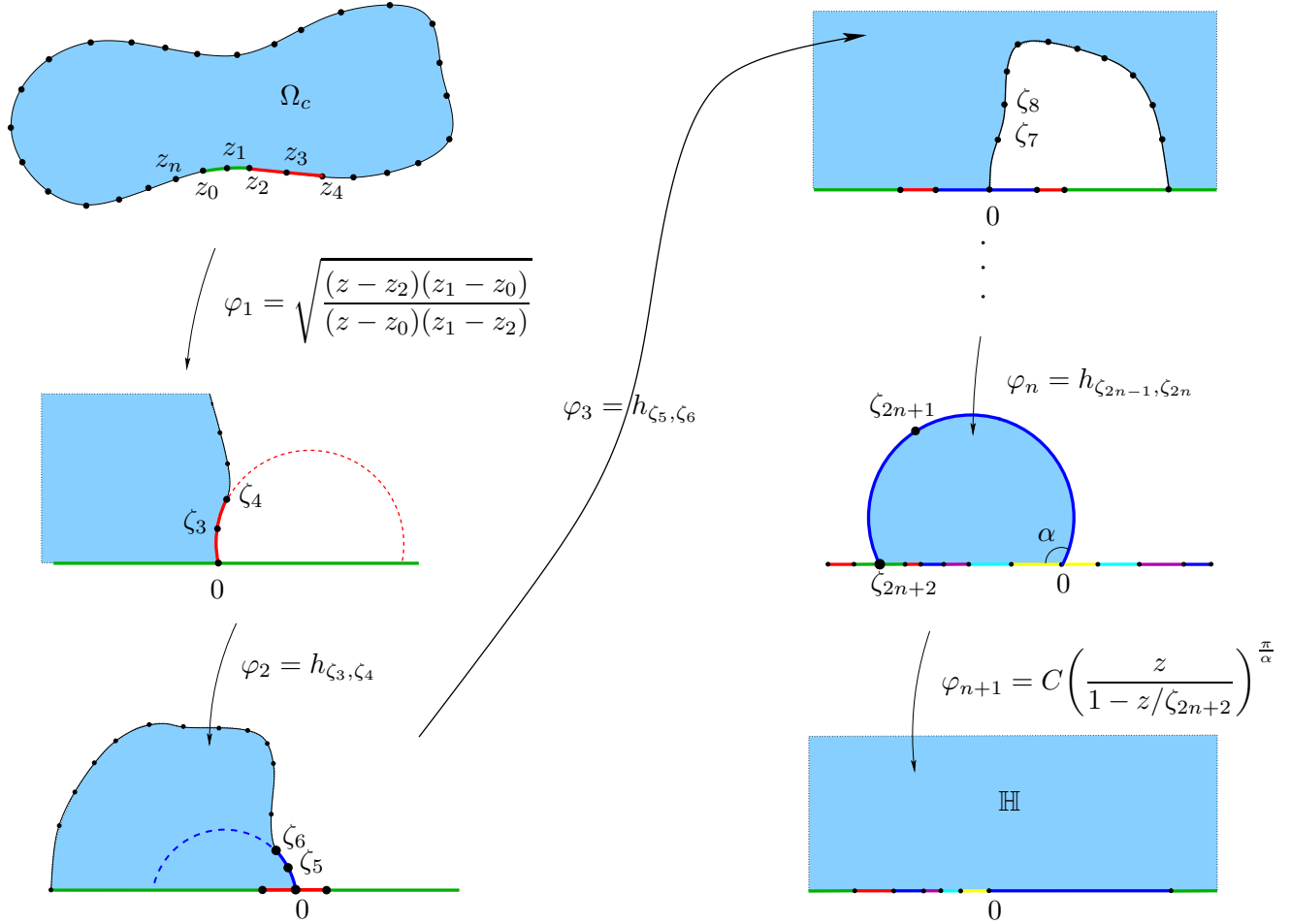


Figure 6. The Zipper Algorithm.

If the zipper algorithm is used to approximate the boundary of a region with bends or angles at some boundary points, then better accuracy is obtained if the bends occur at even numbered vertices $\{z_{2n}\}$.

Conformal Welding

The discovery of the slit algorithm by the first author came from considering conformal weldings. (The simpler geodesic algorithm was discovered later.) A decreasing continuous function $h : [0, +\infty) \rightarrow (-\infty, 0]$ with $h(0) = 0$ is called a **conformal welding** if there is a conformal map f of \mathbb{H} onto $\mathbb{C} \setminus \gamma$ where γ is a Jordan arc from 0 to ∞ such that $f(x) = f(h(x))$ for $x \in \mathbb{R}$. In other words, the map f pastes the negative and positive real half-lines together according to the prescription h to form a curve. One way to approximate a conformal welding is to prescribe the

map h at finitely many points and then construct a conformal mapping of \mathbb{H} which identifies the associated intervals.

A related problem, which the first author considered in joint work with L. Carleson, is: given angles $\alpha_1, \alpha_2, \dots, \alpha_n$ and $0 < x_1 < x_2 < \dots < x_n$, find points $y_n < \dots < y_1 < 0$ so that there is a Schwarz-Christoffel map f of \mathbb{H} onto a region bounded by a polygonal arc tending to ∞ with angles $\alpha_j, 2\pi - \alpha_j$ at the j th vertex $f(x_j) = f(y_j)$. This map welds the intervals $[x_j, x_{j+1}]$ and $[y_{j+1}, y_j]$, $j = 1, \dots, n$. Unfortunately, at the time the best Schwarz-Christoffel method was only fast enough to do this problem with polygonal curves with up to 20 bends.

The basic maps g_a can be used to compute the conformal maps of weldings. Indeed, suppose $y_1 < 0 < x_1$, let $a = x_1/(x_1 - y_1)$, and apply the map $g_a(z/(x_1 - y_1))$. This map identifies the intervals $[y_1, 0]$ and $[0, x_1]$, by mapping them to the two “sides” of a line segment $L \subset \mathbb{H}$. Composing maps of this form will give a conformal map $\varphi : \mathbb{H} \rightarrow \mathbb{C} \setminus \gamma$ such that $\varphi([x_j, x_{j+1}]) = \varphi([y_{j+1}, y_j])$. The final intervals are welded together using the map z^2 . The numerical computation of these maps is easily fast enough to compose 10^5 basic maps, thereby giving an approximation to almost any conformal welding. Conversely, given a Jordan arc γ connecting 0 to ∞ , the associated welding can be found approximately by using the slit algorithm to approximate the conformal map from \mathbb{H} to the complement of γ .

The idea of closing up such a region using a map of the form φ_{n+1} was suggested by L. Carleson, for which we thank him.

Since we have been asked about this a couple of times, we note that conformal welding can also be defined using the conformal maps to the inside and outside of a closed Jordan curve. If f is a conformal map of the unit disc \mathbb{D} onto a Jordan region Ω and if g is a conformal map of $\mathbb{C} \setminus \overline{\mathbb{D}}$ onto $\mathbb{C} \setminus \overline{\Omega}$ which maps ∞ to ∞ then f and g extend to be homeomorphisms of $\overline{\mathbb{D}}$ onto $\overline{\Omega}$ and $\mathbb{C} \setminus \mathbb{D}$ onto $\mathbb{C} \setminus \Omega$ respectively. Then the map

$$h = f^{-1} \circ g : \partial\mathbb{D} \longrightarrow \partial\mathbb{D}$$

is a homeomorphism of the unit circle and is also called a conformal welding. Again, if we approximate a homeomorphism h by prescribing it at finitely many points on the circle, then we can use the slit algorithm to identify the corresponding intervals. Simply map the disc to the upper-half plane so that the first interval I is mapped to \mathbb{R}^+ , the positive reals, and map the complement of the disc to the lower half plane so that desired image $h(I)$ is mapped to \mathbb{R}^+ . Apply $i\sqrt{z}$ and now proceed to identify the remaining intervals as above. Conformal welding can also be accomplished using the geodesic algorithm. We leave the elementary details to the interested reader.

From this point of view, the slit or the geodesic algorithms find the conformal welding of a curve (approximately). From the point of view of increasing the boundary via a small curve γ_j from z_j to z_{j+1} , the algorithms are discrete solutions of Löwner's differential equation.

§2. Disc-chains

The geodesic algorithm can be applied to any sequence of data points z_0, z_1, \dots, z_n , unless the points are out of order in the sense that a data point z_j belongs to the geodesic from z_{k-1} to z_k , for some $k < j$. In this section we will give a simple condition on the data points z_0, z_1, \dots, z_n which is sufficient to guarantee that the curve computed by the geodesic algorithm is close to the polygon with vertices $\{z_j\}$.

Definition 2.1. A **disc-chain** D_0, D_1, \dots, D_n is a sequence of pairwise disjoint open discs such that ∂D_j is tangent to ∂D_{j+1} , for $j = 0, \dots, n-1$. A **closed disc-chain** is a disc-chain such that ∂D_n is tangent to ∂D_0 .

Any closed Jordan polygon P , for example, can be covered by a closed disc-chain with arbitrarily small radii and centers on P . There are several ways to accomplish this, but one straightforward method is the following: Given $\varepsilon > 0$, find pairwise disjoint discs $\{B_j\}$ centered at each vertex, and of radius less than ε . Then

$$P \setminus \bigcup_j B_j = \bigcup L_k$$

where $\{L_k\}$ are pairwise disjoint closed line segments. Cover each L_k with a disc-chain centered on L_k tangent to the corresponding B_j at the ends, and radius less than half the distance to any other L_i , and less than ε .

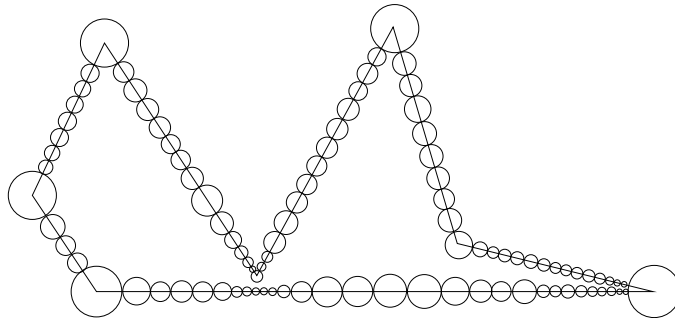


Figure 7. Disc-chain covering a polygon.

Another method for constructing a disc-chain is to use a Whitney decomposition of a simply connected domain. Suppose Ω is a simply connected domain contained in the unit square. The square is subdivided into 4 equal squares. Each of these squares is subdivided again into 4 equal squares, and the process is repeated. If Q is a square, let $2Q$ denote the square with the same center, and sides twice as long. In the subdivision process, if a square Q satisfies $2Q \subset \Omega$, then no further subdivisions are made in Q . Let U_n be the union of all squares Q obtained by this process with side length at least 2^{-n} for which $2Q \subset \Omega$. If $z_0 \in \Omega$, let Ω_n be the component of the interior of U_n containing z_0 . Then $\partial\Omega_n$ is a polygonal Jordan curve. Note that $\partial\Omega_n$ consists of sides of squares Q with length 2^{-n} . Thus we can form a disc chain by placing a disc of radius $2^{-n}/2$ at each vertex of $\partial\Omega_n$. The points of tangency are the midpoints of each square with edge length 2^{-n} on $\partial\Omega_n$.

Yet another method for constructing a disc-chain would be to start with a hexagonal grid of tangent discs, all of the same size, then select a sequence of these discs which form a disc-chain. The boundary circles of a circle packing of a simply connected domain can also be used to form a disc-chain. See for example any of the pictures in Stephenson [SK].

If D_0, D_1, \dots, D_n is a closed disc-chain, set

$$z_j = \partial D_j \cap \partial D_{j+1},$$

for $j = 0, \dots, n$, where $D_{n+1} \equiv D_0$.

Theorem 2.2. *If D_0, D_1, \dots, D_n is a closed disc-chain, then the geodesic algorithm applied to the data z_0, z_1, \dots, z_n produces a conformal map φ_c^{-1} from the upper half plane \mathbb{H} to a region bounded by a C^1 and piecewise analytic Jordan curve γ with*

$$\gamma \subset \bigcup_0^n (D_j \cup z_j).$$

Proof. An arc of a circle which is orthogonal to \mathbb{R} is a hyperbolic geodesic in the upper half plane \mathbb{H} . Let γ_j denote the portion of the computed boundary, $\partial\Omega_c$, between z_j and z_{j+1} . Since hyperbolic geodesics are preserved by conformal maps, γ_j is a hyperbolic geodesic in

$$\mathbb{C}^* \setminus \bigcup_{k=0}^{j-1} \gamma_k.$$

For this reason, we call the algorithm the “geodesic” algorithm.

Using the notation of Figure 2, each map f_a^{-1} is analytic across $\mathbb{R} \setminus \{\pm c\}$, where $f_a(\pm c) = 0$, and f_a^{-1} is approximated by a square root near $\pm c$. If f_b^{-1} is another basic map, then f_b^{-1} is analytic and asymptotic to a multiple of z^2 near 0. Thus $f_b^{-1} \circ f_a^{-1}$ preserves angles at $\pm c$. The geodesic γ_j then is an analytic arc which meets γ_{j-1} at z_j with angle π . Thus the computed boundary $\partial\Omega$ is C^1 and piecewise analytic. The first arc γ_0 is a chord of D_0 and hence not tangent to ∂D_0 . Since the angle at z_1 between γ_0 and γ_1 is π , γ_1 must enter D_1 , and so by Jørgensen's theorem (see Theorem A.1 in the appendix)

$$\gamma_1 \subset D_1,$$

and γ_1 is not tangent to ∂D_1 . By induction

$$\gamma_j \subset D_j,$$

$$j = 0, 1, \dots, n. \quad \blacksquare$$

Disc-chains can be used to approximate the boundary of an arbitrary simply connected domain.

Lemma 2.3. *Suppose that Ω is a bounded simply connected domain. If $\varepsilon > 0$, then there is a disc-chain D_0, \dots, D_n so that the radius of each D_j is at most ε and $\partial\Omega$ is contained in an ε -neighborhood of $\cup D_j$.*

Proof. We may suppose that Ω is contained in the unit square. Then for n sufficiently large, the disc chain constructed using the Whitney squares with side length at least 2^{-n} , as described above, satisfies the conclusions of Lemma 2.3. ■

The **Hausdorff distance** d_H in a metric ρ between two sets A and B is the smallest number d such that every point of A is within ρ -distance d of B , and every point of B is within ρ -distance d of A . The ρ -metrics we will consider in this article are the Euclidean and spherical metrics.

A consequence is the following theorem.

Theorem 2.4. *If Ω is a bounded simply connected domain then for any $\varepsilon > 0$, the geodesic algorithm can be used to find a conformal map f_c of \mathbb{D} onto a Jordan region Ω_c so that*

$$d_H(\partial\Omega, \partial\Omega_c) < \varepsilon, \tag{2.1}$$

where d_H is the Hausdorff distance in the Euclidean metric. If $\partial\Omega$ is a Jordan curve then we can find f_c so that

$$\sup_{z \in \overline{\mathbb{D}}} |f(z) - f_c(z)| < \varepsilon,$$

where f is a conformal map of \mathbb{D} onto Ω .

Proof. The first statement follows immediately from Theorem 2.2 and Lemma 2.3. To prove the second statement, note that the boundary of the regions constructed with the Whitney decomposition converges to $\partial\Omega$ in the Fréchet sense. By a theorem of Courant [T, page 383], the mapping functions can be chosen to be uniformly close. ■

We note that if Ω is unbounded, Lemma 2.3 and Theorem 2.4 remain true if we use the spherical metric instead of the Euclidean metric to measure the radii of the discs and the distance to $\partial\Omega$.

There are other ways besides using the Whitney decomposition to approximate the boundary of a region by a disc-chain and hence to approximate the mapping function. However, Theorem 2.4 does not give an explicit estimate of the distance between mapping functions in terms of the geometry of the regions. This issue will be explored in greater detail in Sections 5 and 6.

The von Koch snowflake is an example of a simply connected Jordan domain whose boundary has Hausdorff dimension > 1 . The standard construction of the von Koch snowflake provides a sequence of polygons which approximate it. By Theorem 2.4 the mapping functions constructed from these disc-chains converge uniformly to the conformal map to the snowflake.

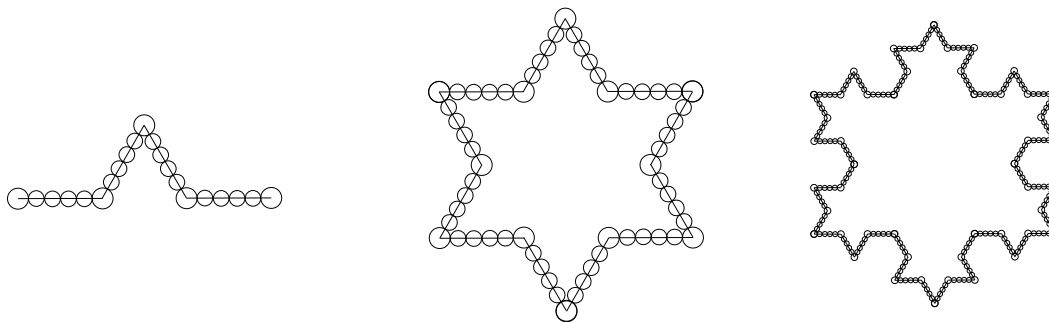


Figure 8. Approximating the von Koch snowflake.

It is somewhat amusing and perhaps known that a constructive proof of the Riemann mapping theorem (without the use of normal families) then follows. Using linear fractional transformations and a square root map, we may suppose Ω is a bounded simply connected domain. Using the disc-chains associated with increasing levels of the Whitney decomposition for instance, Ω can be exhausted by an increasing sequence of domains Ω_n for which the geodesic algorithm can be used to compute the conformal map f_n of Ω_n onto \mathbb{D} with $f_n(z_0) = 0$ and $f'_n(z_0) > 0$. Then by Schwarz's lemma

$$u_n(w) = \log \left| \frac{f_m(w)}{f_n(w)} \right|$$

for $n = m + 1, m + 2, \dots$ is an increasing sequence of positive harmonic functions on Ω_m which is bounded above at z_0 by Schwarz's lemma applied to f_n^{-1} , since Ω is bounded. By Harnack's estimate u_n is bounded on compact subsets of Ω and by the Herglotz integral formula, $\log \frac{f_m(w)}{f_n(w)}$ converges uniformly on closed discs contained in Ω_m . Thus f_n converges uniformly on compact subsets of Ω to an analytic function f . By Hurwitz's theorem f is one-to-one and by Schwarz's lemma applied to f_n^{-1} , f maps Ω onto \mathbb{D} .

In the geodesic algorithm, we have viewed the maps φ_c and φ_c^{-1} as conformal maps between \mathbb{H} and a region Ω_c whose boundary contains the data points. If we are given a region Ω , and choose data points $\{z_k\} \in \partial\Omega$ properly, then the next proposition says that the computed maps φ_c and φ_c^{-1} are also conformal maps between the original region Ω and a region "close" to \mathbb{H} .

Proposition 2.5. *If D_0, \dots, D_n is a closed disc-chain with points of tangency $\{z_k\}$, and if Ω is a simply connected domain such that*

$$\partial\Omega \subset \bigcup_{k=0}^n \overline{D_k}$$

then the computed map φ_c for the data points $\{z_k\}_0^n$ extends to be conformal on Ω .

We remark that changing the sign of the last map φ_{n+1} in the construction of φ_c gives a conformal map of the complement of the computed region onto \mathbb{H} . We choose the sign so that the computed boundary winds once around a given interior point of Ω .

Proof. Without loss of generality $\Omega \supset \bigcup_{k=0}^n D_k$ and hence $\partial\Omega \subset \cup \partial D_k$. The basic map f_a in Figure 2 extends by reflection to be a conformal map of $\mathbb{C}^* \setminus (\gamma \cup \gamma^R)$ onto $\mathbb{C}^* \setminus [-c, c]$, where γ^R is the reflection of γ about \mathbb{R} . In fact, if $\sigma \subset \mathbb{H}$ is any connected set such that $0, a \in \overline{\sigma}$ then f_a is conformal on $\mathbb{C}^* \setminus (\sigma \cup \sigma^R)$, where σ^R is the reflection of σ about \mathbb{R} . In particular, if U is a simply connected region contained in \mathbb{H} with $0, a \in \partial U$, then $\mathbb{C} \setminus \overline{f_a(U \cup U^R)}$ consists of two open sets

$V \cup -V$ where $(0, c) \in V$ and $(0, -c) \in -V$. Here U^R denotes the reflection of the set U about \mathbb{R} and $-V = \{-z : z \in V\}$.

Set

$$\psi_k \equiv \varphi_k \circ \cdots \circ \varphi_1$$

and

$$W_k = \psi_k(\mathbb{C}^* \setminus \{D_0 \cup \dots \cup D_n\}).$$

Then we claim $\mathbb{C}^* \setminus \{W_k \cup W_k^R\}$ consists of $2(n+1)$ pairwise disjoint simply connected regions:

$$\mathbb{C}^* \setminus \{W_k \cup W_k^R\} = \bigcup_{j=k}^n \psi_k(D_j) \cup \psi_k(D_j)^R \cup \bigcup_{j=1}^{2k} U_{k,j},$$

where each region $U_{k,j}$ is symmetric about \mathbb{R} and $\mathbb{R} \subset \cup_{j=1}^{2k} \overline{U_{k,j}}$. The case $k=1$ follows since $\psi_1(\mathbb{C}^* \setminus D_0)$ is bounded by two lines from 0 to ∞ . As noted above, the image of $\psi_{k-1}(D_{k-1}) \cup \psi_{k-1}(D_{k-1})^R$ by the map φ_k consists of two regions V and $-V$. The claim now follows by induction. Note $\delta_k = \psi_k(\partial\Omega \cap \partial D_{k-1})$ is a simple curve connecting a point $-c_k$ to 0 and 0 to c_k , satisfying $z \in \delta_k$ if and only if $-z \in \delta_k$, since $\sqrt{z^2+1}$ is odd. Since each φ_k extends to be one-to-one and analytic on $\psi_{k-1}(D_{k-1})$ and since $U_{n,j}$, $j=1, \dots, 2n$ are disjoint, the map ψ_n is one-to-one and analytic on Ω . By direct inspection, the final map φ_{n+1} extends to be one-to-one and analytic, completing the proof of Proposition 2.5 ■

As one might surmise from the proof of Proposition 2.5, care must be taken in any numerical implementation to assure that the proper branch of $\sqrt{z^2+c^2}$ is chosen at each stage in order to find the analytic extension of the computed map to all of Ω .

§3. Diamond-chains and Pacmen

If we have more control than the disc-chain condition on the behavior of the boundary of a region, then we show in this section that the geodesic algorithm approximates the boundary with better estimates. We will first restrict our attention to domains of the form $\mathbb{C} \setminus \gamma$ where γ is a Jordan arc tending to ∞ .

Definition 3.1. An ε -**diamond** $D(a, b)$ is an open rhombus with opposite vertices a and b and interior angle 2ε at a and at b . If $a = \infty$, then an ε -**diamond** $D(\infty, b)$ is a sector $\{z :$

$|\arg(z - b) - \theta| < \varepsilon$. An ε -**diamond-chain** is a pairwise disjoint sequence of ε -diamonds $D(z_0, z_1), D(z_1, z_2), \dots, D(z_{n-1}, z_n)$. A **closed ε -diamond-chain** is an ε -diamond-chain with $z_n = z_0$.

See Figure 9. Let $B(z, R)$ denote the disc centered at z with radius R .

Definition 3.2. A **pacman** is a region of the form

$$P = B(z_0, R) \setminus \{z : |\arg(\bar{\lambda}(z - z_0))| \leq \varepsilon\},$$

for some **radius** $R < \infty$, **center** z_0 , **opening** $2\varepsilon > 0$, and **rotation** λ , $|\lambda| = 1$.

Let C_1 be a constant to be chosen later (see Lemma 3.7), and let $z_0 = \infty$.

Definition 3.3. We say that an ε -diamond-chain $D(\infty, z_1), D(z_1, z_2), \dots, D(z_{n-1}, z_n)$, satisfies the ε -**pacman condition** if for each $1 \leq k \leq n - 1$ the pacman

$$P_k = B(z_k, R_k) \setminus \{z : |\arg\left(\frac{z - z_k}{z_k - z_{k+1}}\right)| \leq \varepsilon\},$$

with radius $R_k = C_1|z_{k+1} - z_k|/\varepsilon^2$ satisfies

$$\left(\bigcup_{j=0}^{k-2} D(z_j, z_{j+1})\right) \cap P_k = \emptyset.$$

The pacman P_k in Definition 3.3 is chosen to be symmetric about the segment between z_k and z_{k+1} with opening 2ε equal to the interior angle 2ε in the diamond-chain. Note that the ε -diamond $D(z_{k-1}, z_k)$ may intersect P_k .

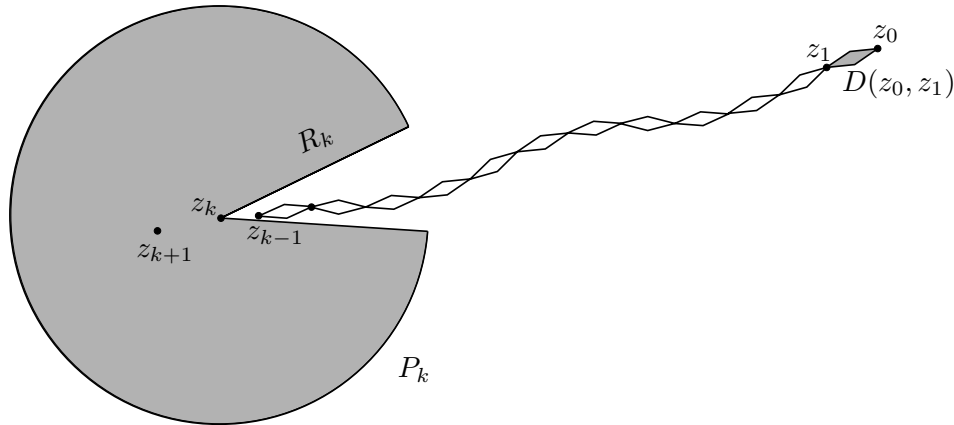


Figure 9. A Diamond-chain and a Pacman.

When $z_0 = \infty$, the first map in the geodesic algorithm is replaced by $\varphi_1(z) = \lambda\sqrt{z - z_1}$. The argument of λ can be chosen so that $\varphi_1(z_2)$ is purely imaginary, in which case the boundary of the constructed region contains the half-line from z_2 through z_1 and ∞ . We will henceforth assume that

$$D(\infty, z_1) = \{z : |\arg\left(\frac{z - z_1}{z_1 - z_2}\right)| < \varepsilon\}.$$

Theorem 3.4. *There exist universal constants $\varepsilon_0 > 0$ and C_1 such that if an ε -diamond-chain*

$$D(\infty, z_1), D(z_1, z_2), \dots, D(z_{n-1}, z_n)$$

satisfies the ε -pacman condition with $\varepsilon < \varepsilon_0$, and if

$$\left| \arg\left(\frac{z_{k+1} - z_k}{z_k - z_{k-1}}\right) \right| < \frac{\varepsilon}{10}, \quad (3.1)$$

for $k = 2, \dots, n-1$, then the boundary curve γ computed by the geodesic algorithm with the data $z_0 = \infty, z_1, \dots, z_n$ satisfies

$$\gamma \subset \bigcup_{k=1}^n \left(D(z_{k-1}, z_k) \cup \{z_k\} \right).$$

Moreover, the argument θ of the tangent to γ between z_k and z_{k+1} satisfies $|\theta - \arg(z_{k+1} - z_k)| < 3\varepsilon$.

To prove Theorem 3.4, we first give several lemmas.

Lemma 3.5. *There exists $\varepsilon_0 > 0$ such that if $\varepsilon < \varepsilon_0$, and if Ω is a simply connected region bounded by a Jordan arc $\partial\Omega$ from 0 to ∞ with*

$$\{z : |\arg z| < \pi - \varepsilon\} \subset \Omega,$$

then the conformal map f of $\mathbb{H}^+ = \{z : \operatorname{Re} z > 0\}$ onto Ω normalized so that $f(0) = 0$ and $f(\infty) = \infty$ satisfies

$$|\arg z_0^2 f'(z_0)| < \frac{5\varepsilon}{6}, \quad (3.2)$$

where $z_0 = f^{-1}(1)$.

The circle C_{z_0} which is orthogonal to the imaginary axis at 0 and passes through z_0 has a tangent vector at z_0 with argument equal to $2\arg z_0$. The quantity $\arg z_0^2 f'(z_0)$ in (3.2) is the argument of the tangent vector to $f(C_{z_0})$ at $f(z_0)$.

Proof. We may suppose that $|z_0| = 1$. Set

$$g(z) = \log \frac{f(z)}{z^2}.$$

Then $|\operatorname{Im}g(z)| \leq \varepsilon$ on $\partial\mathbb{H}^+$ and hence also on \mathbb{H}^+ , and $|\arg z_0| \leq \frac{\varepsilon}{2}$, since $f(z_0) = 1$. Set $\alpha = \frac{\pi}{2\varepsilon}$ and

$$A = e^{\alpha g(z_0)} = z_0^{-2\alpha},$$

$$\varphi(z) = \frac{e^{\alpha z} - A}{e^{\alpha z} + A},$$

and

$$\tau(z) = \frac{1+z}{1-z} \operatorname{Re}z_0 + i\operatorname{Im}z_0.$$

Then τ is a conformal map of \mathbb{D} onto \mathbb{H}^+ such that $\tau(0) = z_0$ and φ is a conformal map of the strip $\{|\operatorname{Im}z| < \varepsilon\}$ onto \mathbb{D} so that $\varphi(g(z_0)) = 0$. Thus $h = \varphi \circ g \circ \tau$ is analytic on \mathbb{D} , bounded by 1 and $h(0) = 0$, so that by Schwarz's lemma

$$|\varphi'(g(z_0))||g'(z_0)||\tau'(0)| = |h'(0)| \leq 1.$$

Consequently

$$\left| \frac{f'(z_0)}{f(z_0)} - \frac{2}{z_0} \right| = |g'(z_0)| \leq \frac{2\varepsilon|\operatorname{Re}A|}{\pi \operatorname{Re}z_0} \leq \frac{2\varepsilon}{\pi \cos \frac{\varepsilon}{2}},$$

and hence

$$\begin{aligned} |\arg z_0^2 f'(z_0)| &= \left| \arg z_0 + \arg \frac{z_0 f'(z_0)}{f(z_0)} \right| \\ &\leq \frac{\varepsilon}{2} + \sin^{-1} \left(\frac{\varepsilon}{\pi \cos \frac{\varepsilon}{2}} \right) \\ &= \left(\frac{1}{2} + \frac{1}{\pi} \right) \varepsilon + O(\varepsilon^2). \end{aligned}$$

This proves Lemma 3.5 if ε is sufficiently small. ■

Lemma 3.6. *Let Ω satisfy the hypotheses of Lemma 3.5. If $\varepsilon < \varepsilon_0/2$, then the hyperbolic geodesic γ from 0 to 1 for the region Ω lies in the kite*

$$P = \{z : |\arg z| < \varepsilon\} \cap \{z : |\arg(1-z)| < \frac{5\varepsilon}{6}\},$$

and the tangent vectors to γ have argument less than $\frac{8}{3}\varepsilon$.

Proof. By Jørgensen's theorem, γ is contained in the closed disc through 1 and 0 which has slope $\tan \varepsilon$ at 0. Likewise γ is contained in the reflection of this disc about \mathbb{R} and hence $|\arg z| < \varepsilon$ on

γ . This also shows that γ is contained in a kite like P but with angles ε at both 0 and 1. In the proof of Theorem 3.4, however, we need the improvement to $\frac{5\varepsilon}{6}$ of the angle at 1.

By Lemma 3.5, a portion of γ near 1 lies in P . Suppose $w_1 \in \gamma$ with $|\arg w_1| = \delta < \varepsilon$ and then apply Lemma 3.5 to the region $\frac{1}{w_1}\Omega$ with ε replaced by $\varepsilon + \delta$. Then the tangent vector to γ at w_1 has argument θ where

$$|\theta - \arg w_1| < \frac{5}{6}(\varepsilon + |\arg w_1|). \quad (3.3)$$

Since $|\arg w_1| < \varepsilon$, we have $|\theta| \leq \frac{8}{3}\varepsilon$. Moreover (3.3) also implies $\theta < \frac{5}{6}\varepsilon$, when $\arg w_1 \leq 0$, and $\theta > -\frac{5}{6}\varepsilon$ when $\arg w_1 \geq 0$. But if w_1 is the last point on $\gamma \cap \partial P$ before reaching 1, this is impossible. Thus $\gamma \subset P$, proving the lemma. \blacksquare

The next lemma improves Lemma 3.5 by only requiring that the portion of $\partial\Omega$ in a large disc lies inside a small sector.

Lemma 3.7. *There is a constant C_1 so that if $\varepsilon < \varepsilon_0/2$ and if $\partial\Omega$ is a Jordan arc such that $0 \in \partial\Omega$, $\partial\Omega \cap \{|z| > C_1/\varepsilon^2\} \neq \emptyset$, and*

$$\{z : |\arg z| < \pi - \varepsilon \text{ and } |z| \leq \frac{C_1}{\varepsilon^2}\} \subset \Omega,$$

then the conformal map $f : \mathbb{H}^+ \rightarrow \Omega$ with $f(0) = 0$ and $|f(\infty)| > \frac{C_1}{\varepsilon^2}$ satisfies

$$|\arg z_0^2 f'(z_0)| < \frac{9\varepsilon}{10}, \quad (3.4)$$

where $z_0 = f^{-1}(1)$.

Proof. As before, we may assume $|z_0| = 1$. Let $\omega(z, E, V)$ denote harmonic measure at z for $E \cap \overline{V}$ in $V \setminus E$. Set $R = \frac{C_1}{\varepsilon^2}$ and $B_R = B(0, R) = \{|z| < R\}$. Then by Beurling's projection theorem and a direct computation

$$\omega(1, \partial B_R, \Omega) \leq \omega(1, \partial B_R, B_R \setminus [-R, 0]) = \frac{4}{\pi} \tan^{-1} \left(\frac{1}{R^{\frac{1}{2}}} \right). \quad (3.5)$$

By the maximum principle

$$\left| \arg \frac{f(z_0)}{z_0^2} \right| \leq \varepsilon + (2\pi + \varepsilon) \frac{4}{\pi} \tan^{-1} \left(\frac{\varepsilon}{C_1^{\frac{1}{2}}} \right) < \frac{11\varepsilon}{10},$$

for C_1 sufficiently large. Since $f(z_0) = 1$,

$$|\arg z_0| \leq \frac{11\varepsilon}{20}. \quad (3.6)$$

Next we show that there is a large half disc contained in $f^{-1}(\Omega \cap B_R)$. Set

$$S = \inf\{|w - i\operatorname{Im}z_0| : w \in \mathbb{H}^+ \text{ and } f(w) \in \partial B_R\}.$$

Using the map

$$\frac{z - i\operatorname{Im}z_0 - S}{z - i\operatorname{Im}z_0 + S}$$

of \mathbb{H}^+ onto \mathbb{D} and Beurling's projection theorem again,

$$\omega(z_0, f^{-1}(\partial B_R), \mathbb{H}^+) \geq \omega(z_0, [S, \infty) + i\operatorname{Im}z_0, \mathbb{H}^+).$$

Then by (3.5), (3.6) and an explicit computation

$$\frac{4}{\pi} \tan^{-1}\left(\frac{\varepsilon}{C_1^{\frac{1}{2}}}\right) \geq \frac{2}{\pi} \tan^{-1}\left(\frac{\operatorname{Re}z_0}{\sqrt{S^2 - \operatorname{Re}z_0^2}}\right).$$

For ε sufficiently small, this implies

$$B(0, \frac{C_1^{\frac{1}{2}}}{2\varepsilon}) \cap \mathbb{H}^+ \subset f^{-1}(\Omega \cap B(0, \frac{C_1}{\varepsilon^2})).$$

Now follow the proof of Lemma 3.5 replacing τ with a conformal map of \mathbb{D} onto $\mathbb{H}^+ \cap \{|z| < \frac{C_1^{\frac{1}{2}}}{2\varepsilon}\}$ such that $\tau(0) = z_0$. Then $\tau'(0) = 2\operatorname{Re}z_0 + O(\frac{\varepsilon}{C_1^{\frac{1}{2}}})$ and for C_1 sufficiently large, (3.4) holds. \blacksquare

Following the proof of Lemma 3.6 (replacing 5/6 by 9/10), the next corollary obtains.

Corollary 3.8. *Suppose $\partial\Omega$ is a Jordan arc such that $0 \in \partial\Omega$, $\partial\Omega \cap \{|z| > C_1/\varepsilon^2\} \neq \emptyset$, and*

$$\{z : |\arg z| < \pi - \varepsilon \text{ and } |z| \leq \frac{C_1}{\varepsilon^2}\} \subset \Omega.$$

If $\varepsilon < \varepsilon_0/2$, then the hyperbolic geodesic γ from 0 to 1 for the region Ω lies in the kite

$$P = \{z : |\arg z| \leq \varepsilon\} \cap \{z : |\arg(1 - z)| \leq \frac{9\varepsilon}{10}\}. \quad (3.7)$$

Moreover, the tangent vectors to this geodesic have argument at most 3ε .

Proof of Theorem 3.4. Use the constant C_1 from Lemma 3.7 in Definition 3.3. As in Theorem 2.2, let γ_j denote the portion of the computed boundary $\partial\Omega$ between z_j and z_{j+1} . By construction $\gamma_0 \cup \gamma_1$ is a half line through $z_0 = \infty$, z_1 , and z_2 . Make the inductive hypotheses that

$$\bigcup_{j=0}^{k-1} \gamma_j \subset \bigcup_{j=0}^{k-1} D(z_j, z_{j+1}) \quad (3.8)$$

and

$$\gamma_{k-1} \cap P_k = \emptyset. \quad (3.9)$$

Since the ε -diamond chain $D(\infty, z_1), D(z_1, z_2), \dots, D(z_{n-1}, z_n)$ satisfies the ε -pacman condition, (3.8) and (3.9) show that the hypotheses of Corollary 3.8 hold for the curve $\gamma = \bigcup_0^{k-1} \gamma_j$ and hence $\gamma_k \subset D(z_k, z_{k+1})$. Also by Corollary 3.8 and (3.1),

$$\gamma_k \cap P_{k+1} = \emptyset.$$

By induction, the theorem follows. ■

If the hypotheses of Theorem 3.4 hold, then the proof of Proposition 2.5 gives the following Corollary.

Corollary 3.9. *If Ω and the diamond chain $D(z_k, z_{k+1})$ satisfy the hypotheses of Theorem 3.4, then the conformal map φ_c computed in the geodesic algorithm extends to be conformal on $\Omega \cup \bigcup_{k=0}^n D(z_k, z_{k+1})$.*

The next Theorem says that for a region Ω bounded by a C^1 curve, the geodesic algorithm with data points z_0, z_1, \dots, z_n produces a region Ω_c whose boundary is a C^1 approximation to $\partial\Omega$.

Theorem 3.10. *Suppose Ω is a Jordan region bounded by a C^1 curve $\partial\Omega$. Then there exists $\delta_0 > 0$, depending on $\partial\Omega$ so that for $\delta < \delta_0$, $\partial\Omega$ is contained in a closed δ -diamond-chain $D = \bigcup D(z_k, z_{k+1})$ and so that $\partial\Omega_c$, the boundary of the region computed by the geodesic algorithm, is contained D . Moreover if $\zeta \in \partial\Omega_c$ and if $\alpha \in \partial\Omega$ with $|\zeta - \alpha| < \delta$ then*

$$|\eta_\zeta - \eta_\alpha| < 6\delta, \quad (3.10)$$

where η_ζ and η_α are the unit tangent vectors to $\partial\Omega$ and $\partial\Omega_c$ at ζ and α , respectively.

Proof. There were two reasons for requiring that $z_0 = \infty$ in Theorem 3.4. The first reason was to assure that

$$\left(\bigcup_0^{k-1} \gamma_j \right) \cap (\mathbb{C} \setminus B(z_k, R_k)) \neq \emptyset \quad (3.11)$$

as needed for Lemma 3.7. The second reason is the difficulty in closing the curve, since Lemma 3.7 does not apply. The difficulty being that a pacman centered at z_n will contain z_0 if z_0 is too close to z_n . Since $\partial\Omega \in C^1$, we may suppose that the δ -diamond chain $D(z_0, z_1), D(z_1, z_2), \dots, D(z_{n-1}, z_n)$ satisfies the pacman condition. Note that this requires z_n to be much closer to z_{n-1} than to z_0 . Since $\partial\Omega \in C^1$, if $|z_n - z_0|$ is sufficiently small, we can find two discs

$$\Delta_p \subset \mathbb{C} \setminus \bigcup_0^{n-1} D(z_k, z_{k+1}),$$

for $p = 1, 2$, with

$$\{z_0, z_n\} = \partial\Delta_1 \cap \partial\Delta_2 \subset \Delta_1 \cap \Delta_2 \subset D(z_n, z_0),$$

where $D(z_n, z_0)$ is a δ -diamond. By Jørgensen's theorem, as in the proof of Theorem 2.2, the geodesic γ_n from z_n to z_0 is contained in $\Delta_1 \cap \Delta_2$. Then by the proof of Theorem 3.4, $\partial\Omega_c$ is contained in the δ -diamond chain. The statement about tangent vectors now follows from Corollary 3.8. ■

We say that $\{z_k\}$ are **locally evenly spaced** if

$$\frac{1}{D} \leq \left| \frac{z_k - z_{k-1}}{z_k - z_{k+1}} \right| \leq D, \quad (3.12)$$

for some constant $D < \infty$. Note that the spacing between points can still grow or decay geometrically. We define the **mesh size** μ of the data points $\{z_j\}$ to be

$$\mu(\{z_j\}) = \sup_k |z_k - z_{k+1}|.$$

We say that a Jordan curve Γ in the extended plane \mathbb{C}^* is a **K -quasicircle** if for some linear fractional transformation τ

$$\frac{|w_1 - w| + |w - w_2|}{|w_1 - w_2|} \leq K \quad (3.13)$$

for all $w_1, w_2 \in \tau(\Gamma)$ and for all w on the subarc of $\tau(\Gamma)$ with smaller diameter. Thus circles and lines are 1-quasicircles. Quasicircles look very flat on all scales if K is close to 1, but for any $K > 1$ they can contain a dense set of spirals. See for example, Figure 8.

If Γ satisfies (3.13) with $K = 1 + \delta$ and small δ and if $\{z_k\} \subset \tau(\Gamma)$ is locally evenly spaced then

$$\left| \arg \left(\frac{z_k - z_{k-1}}{z_{k+1} - z_k} \right) \right| \leq C\delta^{\frac{1}{2}}, \quad (3.14)$$

for some constant C , depending on D .

Theorem 3.11. *There is a constant $K_0 > 1$ so that if Γ is a K -quasicircle with $K = 1 + \delta < K_0$ and if $\{z_k\}$ are locally evenly spaced on Γ , then the geodesic algorithm finds a conformal map of \mathbb{H} onto a region Ω_c bounded by a $C(K)$ -quasicircle containing the data points $\{z_k\}$. The constant $C(K)$ can be chosen so that $C(K) \rightarrow 1$ as $K \rightarrow 1$. Moreover, given $\eta > 0$, if the mesh size $\mu(\{z_k\})$ is sufficiently small then*

$$d_H(\Gamma, \partial\Omega_c) < \eta,$$

where d_H is the Hausdorff distance in the spherical metric.

Proof. We may suppose that Γ satisfies (3.13) with $K = 1 + \delta$ and δ small. Note that $\infty \in \Gamma$. If $\{z_k\}_1^n$ are locally evenly spaced points on $\partial\Omega$, with $\mu = \max |z_k - z_{k-1}|$ sufficiently small then (3.14) holds and $D(\infty, z_1), D(z_1, z_2), \dots, D(z_{n-1}, z_n), D(z_n, \infty)$ is an $C\delta^{\frac{1}{2}}$ -diamond chain, where the main axis of the cone $D(\infty, z_1)$ is in the direction $z_1 - z_2$ and the main axis of $D(z_n, \infty)$ is in the direction $z_n - z_{n-1}$. Moreover $D(\infty, z_1), D(z_1, z_2), \dots, D(z_{n-1}, z_n)$ satisfies the ε -pacman condition if

$$\varepsilon \geq C\delta^{\frac{1}{4}},$$

for some universal constant C . Now apply Theorem 3.4 to obtain $\gamma_j \subset D(z_{j-1}, z_j)$, $j = 1, \dots, n-1$. By an argument similar to the proof of Theorem 3.10, we can also find a geodesic arc for $\mathbb{C} \setminus (\cup_0^{n-1} \gamma_j)$ from z_n to ∞ contained in $D(z_n, \infty)$. Then the computed curve will be a CK -quasicircle. ■

As noted before, the boundary of the region computed with the geodesic algorithm, $\partial\Omega_c$, is a C^1 curve. We end this section by proving that $\partial\Omega_c$ is slightly better than C^1 . If $0 < \alpha < 1$, we say that a curve Γ **belongs to $\mathbf{C}^{1+\alpha}$** if arc length parameterization $\gamma(s)$ of Γ satisfies

$$|\gamma'(s_1) - \gamma'(s_2)| \leq C|s_1 - s_2|^\alpha$$

for some constant $C < \infty$.

We say that a conformal map f defined on a region Ω **belongs to $\mathbf{C}^{1+\alpha}(\overline{\Omega})$** , $0 < \alpha < 1$ provided f and f' extend to be continuous on $\overline{\Omega}$ and there is a constant C so that

$$|f'(z_1) - f'(z_2)| \leq C|z_1 - z_2|^\alpha$$

for all z_1, z_2 in $\overline{\Omega}$.

Proposition 3.12. *If the bounded Jordan region Ω_c is the image of the unit disc by the geodesic algorithm, then*

$$\partial\Omega_c \in C^{3/2},$$

and $\partial\Omega_c \notin C^{1+\alpha}$ for $\alpha > 1/2$, unless Ω_c is a circle or a line. Moreover $\varphi \in C^{3/2}(\overline{\Omega_c})$ and $\varphi^{-1} \in C^{3/2}(\overline{\mathbb{D}})$.

Proof. To prove the first statement, it is enough to show that if γ is an arc of a circle in \mathbb{H} which meets \mathbb{R} orthogonally at 0 (constructed by application of one of the maps f_a^{-1} as in Figure 2), then the curve σ which is the image of $[-1, 1] \cup \gamma$ by the map $S(z) = \sqrt{z^2 - d^2}$ is $C^{\frac{3}{2}}$ (and no better class) in a neighborhood of $S(0) = id$. Indeed, subsequent maps in the composition φ^{-1} are conformal in \mathbb{H} and hence preserve smoothness. For $d > 0$, the function

$$\psi(z) = \sqrt{\left(\frac{\sqrt{z^2 - c^2}}{1 + \sqrt{z^2 - c^2}/b}\right)^2 - d^2} = id + \frac{i}{2d}(z^2 - c^2) - \frac{i}{bd}(z^2 - c^2)^{\frac{3}{2}} + O((z^2 - c^2)^2)$$

for some choice of $b \in \mathbb{R}$ and $c > 0$ is a conformal map of the upper half plane onto a region whose complement contains the curve σ . Clearly $\psi \in C^{\frac{3}{2}}$ near $z = \pm c$, and so by a theorem of Kellogg (see [GM, page 62]), $\sigma \in C^{\frac{3}{2}}$. The same theorem implies σ is not in C^α for $\alpha > \frac{3}{2}$ unless $1/b = 0$. This argument also shows that $\varphi_c \in C^{3/2}(\overline{\Omega})$. To prove $\varphi_c^{-1} \in C^{\frac{3}{2}}(\overline{\mathbb{D}})$, apply the same ideas above to the inverse maps. Alternative, this last fact can be proved by following the proof of Lemma II.4.4 in [GM]. ■

§4. Slits and Newton's method

One complication of the slit and zipper algorithms is that the basic maps $f_a = g_a^{-1}$ cannot be written explicitly in terms of elementary maps, unlike the geodesic algorithm. Newton's method can be used to find the inverse of g_a .

Fix p , with $0 < p < 1$, and let $f(z) = (z - p)^p(z + 1 - p)^{1-p}$. Then $f(\mathbb{H}) = \mathbb{H} \setminus L$ where L is the line segment from 0 to $e^{i\pi p}p^p(1 - p)^{1-p}$. (Note that $\frac{1}{2} \leq |L| \leq 1$). Fix $w \in f(\mathbb{H})$. We wish to solve

$$f(z) = w \tag{4.1}$$

for z . Newton's method then takes an initial guess z_0 and defines

$$z_{n+1} = z_n - \frac{f(z_n) - w}{f'(z_n)}.$$

Near ∞

$$f(z) = z + 1 - 2p + O\left(\frac{1}{z}\right)$$

so a natural first guess for an approximation to the solution z to (4.1) would then be

$$z_0 = w + 2p - 1.$$

The next Theorem says that this initial guess z_0 will work for large w .

Theorem 4.1. *If $0 < p < 1$, set*

$$f(z) = (z - p)^p(z + 1 - p)^{1-p},$$

and suppose $|w| > (1 + \sqrt{5})/2$. Then for $z_0 = w + 2p - 1$ the n -th Newton iterate z_n has relative error

$$\left| \frac{f(z_n) - w}{w} \right| \leq \frac{3}{2} \left(\frac{1}{12} \right)^{2^n}.$$

For example

$$\left| \frac{f(z_4) - w}{w} \right| < 10^{-17}$$

so that z_4 is virtually a formula for $f^{-1}(w)$. In fact, in the slit or geodesic algorithm the points w with small $|w|$ correspond to points in the region near the corresponding vertex, so that most points will have large modulus. In practice, most points need only one or two iterations of Newton's method. The "approximate zero theorem" of Smale and Shub-Smale (see [SS]) can be also used to show that Newton's method will converge quadratically if $|w|$ is sufficiently large. Since we have an explicit formula for f , it is not surprising that we get a somewhat stronger result, in terms of $|w|$, in Theorem 4.1.

Proof. Set $F(z) = (f(z) - w)/w$. We claim that

$$|F(w + 2p - 1)| \leq \frac{p(1-p)}{2} \tag{4.2}$$

and if

$$|F(z)| \leq \frac{p(1-p)}{2}, \tag{4.3}$$

then

$$|z|^2 \geq p(1-p). \quad (4.4)$$

To prove these claims, we study the auxillary function

$$H(\zeta) = (1 - (1-p)\zeta)^p (1 + p\zeta)^{1-p} - 1,$$

which has derivative

$$H'(\zeta) = \frac{p(p-1)\zeta}{[1 + (p-1)\zeta]^{1-p}[1 + p\zeta]^p}.$$

Bounding the denominator from below and integrating we obtain the estimate

$$|H(\zeta)| \leq \frac{p(1-p)}{2} \frac{|\zeta|^2}{1-|\zeta|}. \quad (4.5)$$

Note first that $F(w+2p-1) = H(1/w)$. So that by (4.5)

$$|F(w+2p-1)| \leq \frac{p(1-p)}{2} \left(\frac{2}{1+\sqrt{5}} \right)^2 \frac{1}{1-\frac{2}{1+\sqrt{5}}} = \frac{p(1-p)}{2},$$

proving (4.2).

Suppose now that (4.3) holds and $|z|^2 \leq p(1-p)$. Then

$$1 - \left| \frac{(z-p)^p (z+1-p)^{1-p}}{w} \right| \leq \frac{p(1-p)}{2} \leq \frac{1}{8}.$$

This implies

$$\begin{aligned} |w| &\leq \frac{8}{7} [p^{\frac{1}{2}}(1-p)^{\frac{1}{2}} + p]^p [p^{\frac{1}{2}}(1-p)^{\frac{1}{2}} + 1 - p]^{1-p} \\ &= \frac{8}{7} [p^p (1-p)^{1-p} (1 + 2p^{\frac{1}{2}}(1-p)^{\frac{1}{2}})]^{\frac{1}{2}} \\ &\leq \frac{8\sqrt{2}}{7} < \frac{\sqrt{5}+1}{2}, \end{aligned}$$

contradicting our assumption $|w| \geq (\sqrt{5}+1)/2$, and proving that (4.3) implies (4.4).

Next suppose that (4.3) holds and set

$$\tilde{z} = z - \frac{F(z)}{F'(z)} = z + \left(\frac{z-p}{z} \right) \left[w \left(\frac{z+1-p}{z-p} \right)^p - (z+1-p) \right],$$

Then after some manipulations we obtain the magic formula

$$F(\tilde{z}) = H\left(\frac{F(z)}{z}\right). \quad (4.6)$$

By (4.3) and (4.4),

$$\left| \frac{F(z)}{z} \right| \leq \frac{\sqrt{p(1-p)}}{2} \leq \frac{1}{4},$$

and so by (4.6), (4.5), (4.4) and (4.3)

$$|F(\tilde{z})| \leq \frac{p(1-p)}{2(\frac{3}{4})} \left| \frac{F(z)}{z} \right|^2 \leq \frac{2}{3} |F(z)|^2 < \frac{p(1-p)}{2}$$

By induction and (4.2)

$$\frac{2}{3} |F(z_n)| \leq \left(\frac{2}{3} |F(z_0)| \right)^{2^n} \leq \left(\frac{1}{12} \right)^{2^n},$$

proving Theorem 4.1. ■

The region of possible w where quadratic convergence is obtained can be enlarged with more involved estimates, but Newton's method applied directly to f with this initial value will not always converge. Indeed, the Newton iterate $z - F(z)/F'(z)$ has repelling fixed points at p and $p-1$, and a pole at 0. In order to successfully apply the algorithm to a wide variety of curves we need to find a reliable routine for finding the inverse.

In the implementation of the slit and zipper algorithms we consider four regions based on the length $|L| = p^p(1-p)^{1-p}$ of the segment L and the imaginary part of the tip $w_{\text{tip}} = f(0)$.

$$\begin{aligned} \Omega_\infty &= \{w : |w| \geq \frac{9}{8}|L|\} & \Omega_{\text{tip}} &= \{w : |w - w_{\text{tip}}| < \frac{1}{4}\text{Im}w_{\text{tip}}\} \\ \Omega_p &= \{w : 0 < \arg w < \pi p\} & \Omega_{p-1} &= \{w : \pi p < \arg w < \pi\} \end{aligned}$$

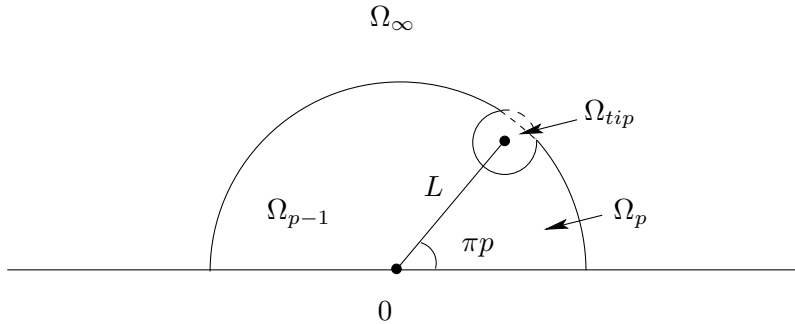


Figure 10. Iteration regions for Newton's method

If $w \in \Omega_\infty$ then we use Newton's method as described in Theorem 4.1. However, we improve the initial guess by taking more terms in the expansion at ∞ :

$$z_0 = w + 2p - 1 + \frac{p(1-p)}{2w} + \frac{(1-2p)p(1-p)}{3w^2},$$

and we rewrite the function to iterate on z/w instead of z to improve numerical accuracy. If $w \notin \Omega_\infty$ but $w \in \Omega_{\text{tip}}$ then we first open up the region by applying $k(w) = \sqrt{w - w_{\text{tip}}}$. Then $k \circ f$ extends to be analytic and one-to-one in a neighborhood of 0. So we use Newton's method to solve $k \circ f(z) = k(w)$ for z . The remaining w are in the sectors between \mathbb{R} and L . If $w \notin \Omega_\infty \cup \Omega_{\text{tip}}$ but $0 < \arg w < \pi p$, then we apply the preliminary map $k_p(z) = z^{\frac{1}{p}}$ instead of k and use Newton's method again. For the remaining points we use the preliminary map $k_{1-p}(z) = z^{\frac{1}{1-p}}$. We leave the proof of the analog of Theorem 4.1 in the remaining three regions to the interested reader. While we cannot prove convergence of Newton's method in every case, extensive numerical testing indicates that we have chosen the proper regions.

§5. Estimates for conformal maps onto nearby domains

We begin this section with a discussion of the following question. Consider two simply connected planar domains Ω_j with $0 \in \Omega_j$ and conformal maps $\varphi_j : \Omega_j \rightarrow \mathbb{D}$ fixing 0, suitably normalized (for instance positive derivative at 0). If Ω_1 and Ω_2 are "close," what can be said about $|\varphi_1 - \varphi_2|$ on $\Omega_1 \cap \Omega_2$, or about $|\varphi_1^{-1} - \varphi_2^{-1}|$ on \mathbb{D} ? The article [W] gives an overview and numerous results in this direction. How should "closeness" of the two domains be measured? Simple examples show that the Hausdorff distance in the Euclidean or spherical metric between the boundaries does not give uniform estimates for either $\|\varphi_1 - \varphi_2\|_\infty$ or $\|\varphi_1^{-1} - \varphi_2^{-1}\|_\infty$.

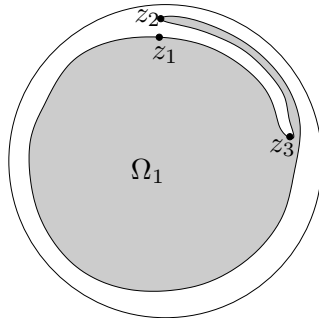


Figure 11. Small Hausdorff distance

For example in Figure 11, Ω_1 contains a disc of radius $1 - \delta$ where δ is small and hence for $\Omega_2 = \mathbb{D}$, $d_H(\Omega_1, \Omega_2) \leq \delta$, but $|\varphi_1(z_1) - \varphi_1(z_2)|$ is large and $|\varphi_1(z_2) - \varphi_1(z_3)|$ is small so that neither $\|\varphi_1(z) - z\|_\infty$ nor $\|\varphi_1^{-1}(z) - z\|_\infty$ is small.

Mainly for ease of notation, we will assume throughout this section that the Ω_j are Jordan domains, and denote $\gamma_j : \partial\mathbb{D} \rightarrow \partial\Omega_j$ an orientation preserving parametrization. Even the more refined distance

$$\inf_{\alpha} \|\gamma_1 - \gamma_2 \circ \alpha\|_\infty,$$

where the infimum is over all homeomorphisms α of $\partial\mathbb{D}$, does not control $\|\varphi_1^{-1} - \varphi_2^{-1}\|_\infty$ or $\|\varphi_1 - \varphi_2\|_\infty$. For example, let Ω_2 be a small rotation of the region Ω_1 in Figure 11. What is needed is some control on the ‘‘roughness’’ of the boundary. Following [W], for a simply connected domain Ω we define

$$\eta(\delta) = \eta_\Omega(\delta) = \sup_C \text{diam } T(C),$$

where the supremum is over all crosscuts of Ω with $\text{diam } C \leq \delta$, and where $T(C)$ is the component of $\Omega \setminus C$ that does not contain 0. Notice that $\eta(\delta) \rightarrow 0$ as $\delta \rightarrow 0$ is equivalent to saying that $\partial\Omega$ is locally connected, and the condition $\eta(\delta) \leq K\delta$ for some constant K is equivalent to saying that Ω is a John-domain (e.g. [P], Chapter 5). It is not difficult to control the modulus of continuity of $\varphi^{-1} : \mathbb{D} \rightarrow \Omega$ in term of η , see [W], Theorem I. This can be used to estimate $\|\varphi_1^{-1} - \varphi_2^{-1}\|_\infty$ in terms of the Hausdorff distance between the boundaries, for example.

Theorem 5.1 (Warschawski[W], Theorem VI). *If Ω_1 and Ω_2 are John-domains, $\eta_j(\delta) \leq \kappa\delta$ for $j = 1, 2$, and if $d_H(\partial\Omega_1, \partial\Omega_2) \leq \epsilon$, then*

$$\|\varphi_1^{-1} - \varphi_2^{-1}\|_\infty \leq C\epsilon^\alpha$$

with $\alpha = \alpha(\kappa)$ and $C = C(\kappa, \text{dist}(0, \partial\Omega_1 \cup \partial\Omega_2))$.

In fact, Warschawski proves that every $\alpha < 2/(\pi^2\kappa^2)$ will work (with $C = C(\alpha)$). Using the Hölder continuity of quasiconformal maps, his proof can easily be modified to give the following better estimate if Ω_1 and Ω_2 are K -quasidisks with K near 1. A K -quasidisk is a Jordan region bounded by a K -quasicircle.

Corollary 5.2. *If Ω_1 and Ω_2 are K -quasidisks, and if $d_H(\partial\Omega_1, \partial\Omega_2) \leq \epsilon$, then*

$$\|\varphi_1^{-1} - \varphi_2^{-1}\|_\infty \leq C\epsilon^\alpha$$

with $\alpha = \alpha(K) \rightarrow 1$ as $K \rightarrow 1$.

As for estimates of $\|\varphi_1 - \varphi_2\|_\infty$, Warschawski shows [W, Theorem VII] that

$$\sup_{\Omega_1} |\varphi_1 - \varphi_2| \leq C\epsilon^{1/2} \log \frac{2}{\epsilon}$$

if $\Omega_1 \subset \Omega_2$, and if Ω_1 is a John-domain, with C depending on κ and on $\text{dist}(0, \partial\Omega_1 \cup \partial\Omega_2)$. However, his result does not apply without the assumption of inclusion $\Omega_1 \subset \Omega_2$. To treat the general case the trick of controlling $|\varphi_1 - \varphi_2|$ by passing to the conformal map φ of the component Ω of $\Omega_1 \cap \Omega_2$ containing 0 (which now is included in Ω_j) does not seem to work, as the geometry of Ω can not be controlled. Nevertheless, for the case of disc-chain domains, the above estimate can be proved, even without any further assumption on the geometry on the circle chain:

Theorem 5.3. *Let D_1, D_2, \dots, D_n be a closed ϵ -disc-chain surrounding 0. Suppose $\partial\Omega_j \subset \cup_k \overline{D_k}$ for $j = 1, 2$, and let $\varphi_j : \Omega_j \rightarrow \mathbb{D}$ be conformal maps with $\varphi_1(0) = \varphi_2(0) = 0$ and $\varphi_1(p) = \varphi_2(p)$ for a point $p \in \partial\Omega_1 \cap \partial\Omega_2$. Then*

$$\sup_{w \in \Omega_1 \cap \Omega_2} |\varphi_1(w) - \varphi_2(w)| \leq C\epsilon^{1/2} \log \frac{1}{\epsilon},$$

where C depends on $\text{dist}(0, \cup_k D_k)$ only.

In case we have control on the geometry of the domains, we have the following counterpart to Corollary 5.2.

Theorem 5.4. *If Ω_1 and Ω_2 are K -quasidisks, if $d_H(\partial\Omega_1, \partial\Omega_2) \leq \epsilon$, and if $\varphi_1(p_1) = \varphi_2(p_2)$ for a pair of points $p_j \in \partial\Omega_j$ with $|p_1 - p_2| \leq \epsilon$, then*

$$\sup_{w \in \Omega} |\varphi_1(w) - \varphi_2(w)| \leq C\epsilon^\alpha$$

with $\alpha = \alpha(K) \rightarrow 1$ as $K \rightarrow 1$, where Ω is the component of $\Omega_1 \cap \Omega_2$ containing 0.

The proofs of both theorems rely on the following harmonic measure estimate, which is an immediate consequence of a theorem of Marchenko [M] (see [W, Section 3], for the statement and a proof). To keep this paper self-contained, we include a simple proof, shown to us by John Garnett, for which we thank him.

Lemma 5.5. *Let $0 < \theta < \pi$, $0 < \epsilon < 1/2$ and set $D = \mathbb{D} \setminus \{re^{it} : -\theta \leq t \leq \theta, 1 - \epsilon \leq r < 1\}$, $A = \partial D \setminus \partial\mathbb{D}$. Then*

$$\omega(0, A, D) \leq \frac{\theta}{\pi} + C\epsilon \log \frac{1}{\epsilon}$$

for some universal constant C .

Proof. Set $\omega(z) = \omega(z, A, D)$ for $z \in D$. By the mean value property, it is enough to show that

$$\omega(z) \leq C \frac{\epsilon}{t - \theta}$$

for $z = (1 - \epsilon)e^{it}$ and $\theta + \epsilon \leq t \leq \pi$. To this end, set $I = \{e^{i\tau} : -\theta \leq \tau \leq \theta\}$ and consider the circular arc $\{\zeta : \omega(\zeta, I, \mathbb{D}) = \frac{1}{3}\}$. If $\epsilon < \epsilon_0$ for some universal ϵ_0 (for $\epsilon \geq \epsilon_0$ there is nothing to prove), then A is disjoint from this arc and it follows that $\omega(\zeta, I, \mathbb{D}) \geq \frac{1}{3}$ on A . The maximum principle implies $\omega(\zeta) \leq 3\omega(\zeta, I, \mathbb{D})$ on D . Now the desired inequality follows from

$$\omega((1 - \epsilon)e^{it}, I, \mathbb{D}) = \frac{1}{2\pi} \int_{-\theta}^{\theta} \frac{1 - (1 - \epsilon)^2}{|(1 - \epsilon)e^{it} - e^{i\tau}|^2} d\tau \leq C\epsilon \int_{-\theta}^{\theta} \frac{1}{(t - \tau)^2} d\tau < C \frac{\epsilon}{t - \theta}. \quad \blacksquare$$

Proof of Theorem 5.3. We may assume that $\varphi_j(p) = 1$. We will first assume that p is one of the points $D_k \cap D_{k+1}$. Denote Ω the largest simply connected domain $\subset \mathbb{C}$ containing 0 whose boundary is contained in $\cup_k D_k$ (thus $\overline{\Omega}$ is the union of $\cup_k D_k$ and the bounded component of $\mathbb{C} \setminus \cup_k D_k$), and φ the conformal map from Ω to \mathbb{D} with $\varphi(0) = 0$ and $\varphi(p) = 1$. First, let $z \in \partial\Omega_1 \cap \partial\Omega$. Denote B respectively B_1 the arc of $\partial\Omega$ ($\partial\Omega_1$) from p to z . By the Beurling projection theorem (or the distortion theorem), every $\varphi(D_j)$ has diameter $\leq C\sqrt{\epsilon}$. Therefore $\varphi(B_1)$ is an arc in $\overline{\mathbb{D}}$, with same endpoints as $\varphi(B)$, that is contained in $S = \{re^{it} : 1 - C\sqrt{\epsilon} \leq r < 1, -C\sqrt{\epsilon} < t < \arg \varphi(z) + C\sqrt{\epsilon}\}$. Denote $A = \partial S$. By Lemma 5.5,

$$\omega(0, B_1, \Omega_1) \leq \omega(0, B_1, \Omega \setminus B_1) \leq \omega(0, A, \mathbb{D} \setminus A) \leq \frac{1}{2\pi} \arg \varphi(z) + 2C\sqrt{\epsilon} + C\sqrt{\epsilon} \log \frac{1}{\sqrt{\epsilon}}$$

and we obtain

$$\arg \varphi_1(z) = 2\pi\omega(0, B_1, \Omega_1) \leq \arg \varphi(z) + C\epsilon^{1/2} \log \frac{1}{\epsilon}.$$

The same argument, applied to the other arc from p to z , gives the opposite inequality, and together it follows that

$$|\varphi(z) - \varphi_1(z)| \leq C\epsilon^{1/2} \log \frac{1}{\epsilon}.$$

Now let $z \in \partial\Omega_1$ be arbitrary. If z' is a point of $\partial\Omega_1 \cap \partial\Omega$ in the same disc D_j as z , then we have

$$|\varphi(z) - \varphi_1(z)| \leq |\varphi(z) - \varphi(z')| + |\varphi(z') - \varphi_1(z')| + |\varphi_1(z) - \varphi_1(z')| \leq 2C\sqrt{\epsilon} + C\epsilon^{1/2} \log \frac{1}{\epsilon}.$$

The maximum principle yields $|\varphi - \varphi_1| \leq C\epsilon^{1/2} \log \frac{1}{\epsilon}$ on Ω_1 . The same argument applies to $|\varphi - \varphi_2|$, and the theorem follows from the triangle inequality.

If $p \in \partial\Omega_1 \cap \partial\Omega_2$ is arbitrary, let p' be one of the points $D_k \cap D_{k+1}$ in the same disc D_j as p . Then the above estimate, applied to a rotation of φ_1, φ_2 and p' gives $|\varphi_2(p')/\varphi_1(p')\varphi_1 - \varphi_2| \leq C\epsilon^{1/2} \log \frac{2}{\epsilon}$ and the theorem follows from $|\varphi_j(p) - \varphi_j(p')| \leq C\sqrt{\epsilon}$. ■

The following lemma is another easy consequence of the aforementioned theorem of Marchenko [M] ([W], Section 3).

Lemma 5.6. *Let $H \subset \mathbb{D}$ be a K -quasidisc with $0 \in H$ such that $\partial H \subset \{1 - \epsilon < |z| < 1\}$, and let h be a conformal map from \mathbb{D} to H with $h(0) = 0$ and $|h(p) - p| < \epsilon$ for some $p \in \partial\mathbb{D}$. Then*

$$|h(z) - z| \leq C\epsilon \log \frac{1}{\epsilon},$$

where C depends on K only.

Proof. We may assume $p = 1$. Let $z = e^{i\tau}$ and consider the arc $A = \{h(e^{it}) : 0 \leq t \leq \tau\} \subset \partial H$ of harmonic measure $\tau/2\pi$. For suitable $C = C(K)$ we have that $D = \mathbb{D} \setminus \{re^{it} : -C\epsilon \leq t \leq \arg h(z) + C\epsilon, 1 - \epsilon \leq r < 1\}$ contains A . By the maximum principle and Lemma 5.5,

$$\tau/2\pi = \omega(0, A, H) \leq \omega(0, \partial D \cap \mathbb{D}, D) \leq \arg h(z)/2\pi + C\epsilon \log \frac{1}{\epsilon}.$$

Applying the same reasoning to $\partial H \setminus A$, the lemma follows for all $z \in \partial\mathbb{D}$ and thus for all $z \in \mathbb{D}$. ■

Note that the conclusion of Lemma 5.6 is true if instead of assuming H is a K -quasidisc, we only assume $\arg z$ is increasing on ∂H .

Proof of Theorem 5.4. Because Ω_1 and Ω_2 are K -quasidisks, φ_1 and φ_2 have K^2 -quasiconformal extensions to \mathbb{C} (see [L], Chapter I.6). In particular, they are Hölder continuous with exponent $1/K^2$ (see [A]), and it follows that with $\alpha = 1/K^2$ and $r = 1 - C\epsilon^\alpha$, we have $\varphi_1^{-1}(\{|z| \leq r\}) \subset \Omega_2$. In particular, $h(z) = \varphi_2(\varphi_1^{-1}(rz))$ is a conformal map from \mathbb{D} onto a K^4 -quasidisc $H \subset \mathbb{D}$, and by the Hölder continuity of φ_2 and φ_1^{-1} we have $\partial H \subset \{1 - C\epsilon^{\alpha^3} < |z| < 1\}$. Now Lemma 5.6 yields $|h(z) - z| \leq C\epsilon^\beta$, for any $\beta < \alpha^3$ and $C = C(\beta)$. For $w \in \Omega \subset \Omega_1 \cap \Omega_2$, let $z = \varphi_1(w)$, then

$$|\varphi_1(w) - \varphi_2(w)| = |z - \varphi_2(\varphi_1^{-1}(z))| \leq |z - \varphi_2(\varphi_1^{-1}(rz))| + |\varphi_2(\varphi_1^{-1}(rz)) - \varphi_2(\varphi_1^{-1}(z))| \leq C\epsilon^\beta,$$

where again we have used the Hölder continuity of φ_2 and φ_1^{-1} . The Theorem follows. ■

§6. Convergence of the Mapping Functions

We will now combine the results of Sections 2 and 3 with the estimates of the previous section, to obtain quantitative estimates on the convergence of the geodesic algorithm. Throughout this section, Ω will denote a given simply connected domain containing 0, bounded by a Jordan curve $\partial\Omega$, z_0, \dots, z_n are consecutive points on $\partial\Omega$, Ω_c is the domain and $\varphi_c : \Omega_c \rightarrow \mathbb{D}$ the map computed by the geodesic algorithm, and $\varphi : \Omega \rightarrow \mathbb{D}$ is a conformal map, normalized so that $\varphi_c(0) = \varphi(0) = 0$ and $\varphi_c(p_0) = \varphi(p_0)$ for some $p_0 \in \partial\Omega \cap \partial\Omega_c$.

Combining Theorems 2.2 and 5.3 and Propositions 2.5 and 3.12 we obtain at once:

Theorem 6.1. *If $\partial\Omega$ is contained in a closed ϵ -disc-chain $\bigcup_{j=0}^n \overline{D_j}$ and if $z_j = \partial D_j \cap \partial D_{j+1}$, then $\partial\Omega_c$ is a smooth ($C^{\frac{3}{2}}$) piecewise analytic Jordan curve contained in $\bigcup_{j=0}^n D_j \cup z_j$, the map φ_c extends to be conformal on $\Omega \cup \Omega_c$ and*

$$\sup_{w \in \Omega} |\varphi(w) - \varphi_c(w)| \leq C\epsilon^{1/2} \log \frac{1}{\epsilon}.$$

Now assume that $\partial\Omega$ is a K -quasicircle with $K < K_0$ and assume approximate equal spacing of the z_j , say, $\frac{1}{2}\epsilon < |z_{j+1} - z_j| < 2\epsilon$. Then

$$\frac{C}{\epsilon} \leq n \leq \frac{C}{\epsilon^d} \tag{6.1}$$

where d (essentially the Minkowski-dimension) is close to 1 when K is close to 1. Combining Theorem 3.11 with Corollary 5.2 and Theorem 5.4, we have:

Theorem 6.2. *Suppose $\partial\Omega$ is a K -quasicircle with $K < K_0$. The Hausdorff distance between $\partial\Omega$ and $\partial\Omega_c$ is bounded by $C(K)\epsilon$, where $C(K)$ tends to 0 as K tends to 1 and n to infinity. Furthermore,*

$$\|\varphi^{-1} - \varphi_c^{-1}\|_{\infty} \leq C\epsilon^{\alpha}$$

and

$$\sup_{w \in \Omega_0} |\varphi(w) - \varphi_c(w)| \leq C\epsilon^{\alpha}$$

with $\alpha = \alpha(K) \rightarrow 1$ as $K \rightarrow 1$, where Ω_0 is the component of $\Omega \cap \Omega_c$ containing 0.

The best possible exponent in (6.1) in terms of the standard definition of $K(\partial\Omega)$, which slightly differs from our geometric definition, is given by Smirnov's (unpublished) proof of Astala's conjecture,

$$d \leq 1 + \left(\frac{K-1}{K+1}\right)^2.$$

This allows us to easily convert estimates given in terms of ε , as in Theorem 6.2, into estimates involving n .

Finally, assume that $\partial\Omega$ is a smooth closed Jordan curve. Then Ω is a K -quasicircle and a John domain by the uniform continuity of the derivative of the arc length parameterization of $\partial\Omega$. The quasiconformal norm $K(\partial\Omega)$ and the John constant depend on the global geometry, as does the ε -pacman condition when there are not very many data points. As the example in Figure 11 shows, even an infinitely differentiable boundary can have a large quasiconformal constant and a large John constant. However, the ε -pacman condition becomes a local condition if the mesh size $\mu(\{z_k\}) = \max_k |z_{k+1} - z_k|$ of the data points is sufficiently small. The radii of the balls in the definition of the ε -pacman condition

$$R_k = C_1 \frac{|z_{k+1} - z_k|}{\varepsilon^2} \tag{6.2}$$

increase as ε decreases, but can be chosen small for a fixed ε if the mesh size μ is small. To apply the geodesic algorithm we suppose that the data points have small mesh size and, as in the proof of Theorem 3.10, $|(z_0 - z_n)/(z_{n-1} - z_n)|$ is sufficiently large so that the ε diamond chain $D(z_0, z_1), \dots, D(z_{n-1}, z_n)$ satisfies the ε -pacman condition and

$$\partial\Omega \subset \bigcup_{k=0}^n D(z_k, z_{k+1})$$

where $D(z_n, z_{n+1}) = D(z_n, z_0)$ is an ε -diamond. This can be accomplished for smooth curves by taking data points z_0, \dots, z_n, z_0 with small mesh size and discarding the last few z_{n-n_1}, \dots, z_n where n_1 is an integer depending on ε and on $\partial\Omega$. The remaining subset still has small mesh size (albeit larger). This process of removing the last few data points is necessary to apply the proof of Theorem 3.10, but in practice it is omitted. We view it only as a defect in the method of proof.

If $\partial\Omega \in C^1$ and if φ is a conformal map of Ω onto \mathbb{D} then $\arg(\varphi^{-1})'$ is continuous. Indeed, it gives the direction of the unit tangent vector. However there are examples of C^1 boundaries

where φ' and $(\varphi^{-1})'$ are not in continuous. In fact it is possible for both to be unbounded. If we make the slightly stronger assumption that $\partial\Omega \in C^{1+\alpha}$ for some $0 < \alpha < 1$, then $\varphi \in C^{1+\alpha}$ and $\varphi^{-1} \in C^{1+\alpha}$ by Kellogg's theorem (see [GM, page 62]). In particular the derivatives are bounded above and below on $\overline{\Omega}$ and $\overline{\mathbb{D}}$, respectively. Because of Proposition 3.12, we will consider the case $1 + \alpha = 3/2$. Similar results are true for $1 + \alpha < 3/2$.

Theorem 6.3. *Suppose $\partial\Omega$ is a closed Jordan curve in $C^{3/2}$ and φ is a conformal map of Ω onto \mathbb{D} . Suppose $z_0, z_1, \dots, z_n, z_0$ are data points on $\partial\Omega$ with mesh size $\mu = \max |z_j - z_{j+1}|$. Then there is a constant C_1 depending on the geometry of $\partial\Omega$, so that the Hausdorff distance between $\partial\Omega$ and $\partial\Omega_c$ satisfies*

$$d_H(\partial\Omega, \partial\Omega_c) \leq C_1 \mu^{3/2} \quad (6.3)$$

and the conformal map φ_c satisfies

$$\|\varphi^{-1} - \varphi_c^{-1}\|_\infty \leq C \mu^p \quad (6.4)$$

and

$$\sup_{z \in \Omega \cap \Omega_c} |\varphi(z) - \varphi_c(z)| \leq C \mu^p, \quad (6.5)$$

for every $p < 3/2$.

For example if n data points are approximately evenly spaced on $\partial\Omega$, so that $\mu = C/n$ then the error estimates are of the form $C/n^{3/2}$ in (6.3) and C/n^p for $p < 3/2$ in (6.4) and (6.5). While Theorem 6.3 gives simple estimates in terms of the mesh size or the number of data points, smaller error estimates can be obtained with fewer data points if the data points are distributed so that there are fewer on subarcs where $\partial\Omega$ is flat and more where the boundary bends or where it folds back on itself. In other words, construct diamond chains with angles ε_k satisfying the ε_k -pacman condition centered at z_k for each k . The errors will then be given by

$$\max_k \left(\varepsilon_k |z_k - z_{k+1}| \right)^p.$$

Proof. It is not hard to see from (6.2) that $\partial\Omega$ satisfies the ε -pacman condition with

$$\varepsilon = C \mu^{1/2},$$

for C sufficiently large. By the proof of Theorem 3.10, $\partial\Omega_c$ is contained in the union of the diamonds. The diamonds $D(z_k, z_{k+1})$ have angle $C\mu^{1/2}$ and width bounded by $C\mu$ and therefore (6.3) holds.

Let ψ be a conformal map of \mathbb{D} onto the complement of $\bar{\Omega}$, $\mathbb{C}^* \setminus \bar{\Omega}$. Then by Kellogg's Theorem as mentioned above, $\psi \in C^{3/2}$. In particular, $|\psi'|$ is bounded above and below on $1/2 < |z| < 1$. By the Koebe distortion theorem there are constants C_1, C_2 so that

$$C_1(1 - |z|) \leq \text{dist}(\psi(z), \partial\Omega) \leq C_2(1 - |z|),$$

for all z with $1/2 < |z| < 1$. Thus we can choose $r = 1 - C_3\mu^{3/2}$ so that the image of the circle of radius r , $I_r = \psi(\{|z| = r\})$, does not intersect the diamond chain and $d_H(I_r, \partial\Omega) \sim \mu^{3/2}$. Then the bounded component of the complement of I_r is a Jordan region U_r containing Ω and bounded by $I_r \in C^{3/2}$, with $C^{3/2}$ norm dependent only on $\partial\Omega$, and the bounds on $|\psi'|$.

Let σ be a conformal map of U_r onto \mathbb{D} . Inequality (6.4) now follows from [W, Theorem VIII] by comparing the conformal maps φ^{-1} and φ_c^{-1} to the conformal map σ^{-1} where $\sigma : U_r \rightarrow \mathbb{D}$ and where all three (inverse) conformal maps are normalized to have positive derivative at 0 and map 0 to the same point in Ω .

To see (6.5), note that

$$\sigma(\partial\Omega \cup \partial\Omega_c) \subset \{z : 1 - |z| < c\mu^{3/2}\}.$$

Moreover, because $\partial\Omega \cup \partial\Omega_c$ is contained in the diamond chain, and because both $\sigma \in C^{3/2}$ and $\sigma^{-1} \in C^{3/2}$, $\arg \sigma(\zeta)$ is increasing along $\partial\Omega$, for μ sufficiently small. By the remark after the proof of Lemma 5.6,

$$|\omega(0, \gamma, \sigma(\Omega)) - \omega(0, \gamma^*, \mathbb{D})| \leq C\mu^{3/2} \log \mu$$

for every subarc γ of $\sigma(\partial\Omega)$, where γ^* denotes the radial projection of γ onto $\partial\mathbb{D}$. The same statements are true for $\partial\Omega_c$. Then (6.5) follows because the harmonic measure of the subarc γ_p of $\partial\Omega$ from p_0 to p is given by

$$\omega(0, \gamma_p, \Omega) = \frac{1}{2\pi} \arg \left(\frac{\varphi(p)}{\varphi(p_0)} \right),$$

and a similar statement is true for φ_c . ■

The constant C in Theorem 6.3 depends on the quasiconformality constant $K(\partial\Omega)$, p , $\text{diam}(\Omega)$, $\text{dist}(0, \partial\Omega)$, and on

$$M = \sup_{1/2 < |z| < 1} (|\psi'|, 1/|\psi'|),$$

where ψ is a conformal map of the complement of Ω to \mathbb{D} . If $I_r = \psi(\{|z| = r\})$ is replaced by a $C^{3/2}$ curve which is constructed geometrically instead of using the conformal map ψ , then the constant C can be taken to depend only on the geometry of the region Ω .

§7. Some Numerical Results

An in depth comparison of the algorithms in this article with other methods of conformal mapping and convergence rates will be written separately. To give the reader a sense of the speed and accuracy of computations, if 10,000 data points are given, it takes about 20 seconds with the geodesic algorithm to compute the mapping functions on an 3.2 GHz Pentium IV computer. Since all of the basic maps are given explicitly in terms of elementary maps, the speed depends only on the number of points, not the shape of the region or the distribution of the data points. The accuracy can be measured if the true conformal map is known. For example

$$f(z) = \frac{rz}{1 + (rz)^2},$$

where $r < 1$ maps the unit disc into an inverted ellipse. See Figure 12. The region was chosen because it almost pinches off at 0, and because the stretching/compression given by $\max|f'|/\min|f'|$ is big for r near 1. Higher resolution images can be obtained from:

<http://www.math.washington.edu/~marshall/preprints/zipper.pdf>

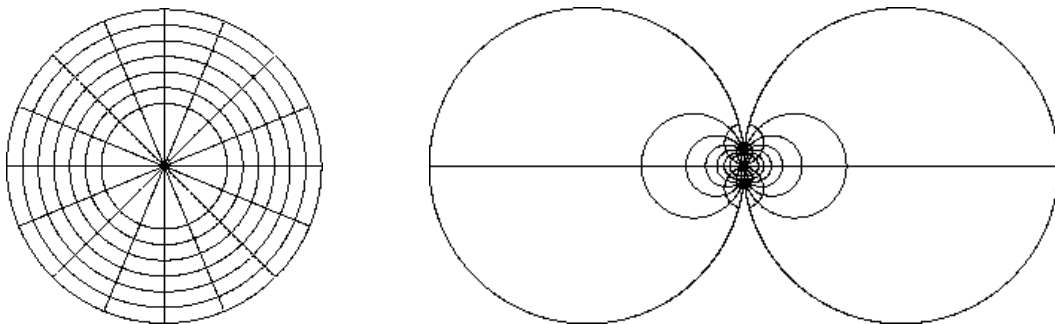


Figure 12. Inverted ellipse with $r = .95$.

We chose $r = .95$ and used as data points the image by f of 10,000 equally spaced points on the unit circle, and compared the corresponding points on the unit circle computed by the geodesic algorithm with 10,000 equally spaced points. The errors were less than $1.8 \cdot 10^{-6}$. The same procedure using the zipper algorithm took 84 seconds, and had errors less than $9.2 \cdot 10^{-8}$. When the number of data points was increased to 100,000, the time to run the geodesic algorithm increased to 25 minutes

with errors less than $2 \cdot 10^{-8}$. In this example, the the difference between successive boundary data points ranged from .025 to $3 \cdot 10^{-6}$ so that perhaps a better distribution of data points would have given smaller errors.

Figure 13 shows the conformal map of a Carleson grid on the disc to both the interior and exterior of the island Tenerife (Canary Islands). The center of the interior is the volcano Teide. It also shows both the original data for the coastline, connected with straight line segments, and the boundary curve connecting the data points using the zipper algorithm. At this resolution, it is not possible to see the difference between these curves. The zipper algorithm was applied to 6,168 data points and took 36 seconds. The image of 24,673 points on the unit circle took 48 seconds and all of these points were within $9 \cdot 10^{-5}$ of the polygon formed by connecting the 6,168 data points. The points on the circle corresponding to the 6,168 vertices were mapped to points within 10^{-10} of the vertices. This error is due to the tolerance set for Newton's method, round-off error, and the compression/expansion of harmonic measure. The image of 8,160 vertices in the Carleson grid took 25 seconds to be mapped to the interior and 25 seconds to the exterior.

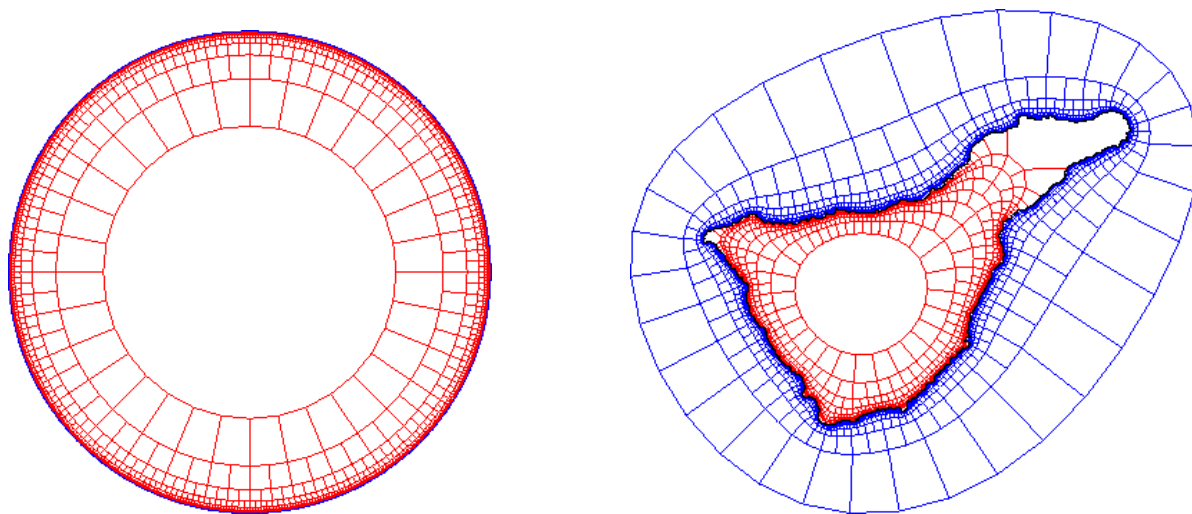


Figure 13. Tenerife.

Higher resolution images can be obtained from:

<http://www.math.washington.edu/~marshall/preprints/zipper.pdf>

The first objection one might have in applying these algorithms with a large number of data points is that compositions of even very simple analytic maps can be quite chaotic. Indeed this is the subject of the field complex dynamics. We could redefine the basic maps f_a by composing with a linear fractional transformation of the upper half plane so that the composed map is asymptotic to z as $z \rightarrow \infty$. This will not affect the computed curve in these algorithms since the next basic

map begins with a linear fractional transformation (albeit altered). However, if we formulate the basic maps in this way, then because the maps are nearly linear near ∞ , the numerical errors will accumulate only linearly.

Osculation methods also approximate a conformal map by repeated composition of simple maps. See Henrici [H] for a discussion of osculation methods and uniform convergence on compact sets. The algorithms of the present article follow the boundary of a given region much more closely than, for instance, the Koebe algorithm and give uniform convergence rather than just uniform on compacta. It is possible to use the techniques of this paper to prove the geodesic algorithm is an osculation method for smooth curves, and therefore by the results in [H] converge uniformly on compact subsets. However, prior to this article even a proof that these methods satisfied the osculation family conditions was not known.

Recently Banjai and Trefethen [BT] adapted multigrid techniques to the Schwarz-Christoffel algorithm and successfully computed the conformal map to a region bounded by a polygon with about 10^5 edges. They used a 12 fold symmetry in the region to immediately reduce the parameter problem to size 10^4 . Any other conformal mapping technique can also use symmetry and obtain a 12 fold reduction in the number of data points required, however their work does show at least that Schwarz-Christoffel is possible with 10^4 vertices, though convergence of the algorithm to solve the parameter problem is not always assured. The zipper algorithm is competitive in speed and accuracy for such regions. The geodesic algorithm is almost as good, and has the advantage that it is very easy to code and convergence can be proved. It would be interesting to try to prove convergence of the technique used in [BT] to find the prevertices, for polygons which are K -quasicircles in terms of K . It would be interesting as well to apply multigrid techniques to the zipper algorithm.

One additional observation worth repeating in this context is that the geodesic and zipper algorithms *always* compute a conformal map of \mathbb{H} to a region bounded by a Jordan curve passing through the data points, even if the disc-chain or pacman conditions are not met. The image region can be found by evaluating the function at a large number of points on the real line. By Proposition 2.5 and Corollary 3.9, if the data points $\{z_j\}$ satisfy the hypotheses of Theorem 2.2 or Theorem 3.4, then φ can be analytically extended to be a conformal map of the original region Ω to a region very close to \mathbb{D} . To do so requires careful consideration of the appropriate branch of \sqrt{z} at each stage of the composition.

Theorem 2.2 and Theorem 3.4 and their proofs suggest how to select points on the boundary of a region to give good accuracy for the mapping functions. Roughly speaking, points need to be chosen closer together where the region comes close to folding back on itself. See Figure 12

for example. Greater accuracy can be obtained by placing more points on the boundary near the center and fewer on the big lobes. See also the remarks after the statement of Theorem 6.3 in this regard. In practice, the zipper map works well if points are distributed so that

$$B(z_k, 5|z_{k+1} - z_k|) \cap \partial\Omega \tag{7.1}$$

is connected.

When the boundary of the given region is not smooth, then one of the processes described in section 2 should be used to generate the boundary data, if the geodesic algorithm is to be used. For example, if nothing is known about the boundary except for a list of data points, then we preprocess the data by taking data points along the line segments between the original data points, so that these new points correspond to points of tangency of disjoint circles centered on the line segments, including circles centered at the original data points. Note that the original boundary points are not among these new data points. The geodesic algorithm then finds a conformal map to a region with the new data points on the boundary. The boundary of the new region will be close to the polygonal curve through the original data points, but will not pass through the original data points. This boundary is “rounded” near the original data points. Indeed it is a smooth curve.

When the boundary of the desired region is less smooth, for example with “corners”, then the zipper or slit algorithms should be used. In this case additional points are placed along the line segments between the data points, with at least 5 points per edge and satisfying (7.1). In practice, at least 500 points are chosen on the boundary so that the image of the circle will be close to the polygonal line through the data points. Since two data points are pulled down to the real line with each basic map in the zipper algorithm, the original data points should occur at even numbered indices in the resulting data set (the first data point is called z_0). Then the computed boundary Ω_c will have corners at each of the original data points, with angles very close to the angles of the polygon through the original data points.

A version of the zipper algorithm can be obtained from [MD]. The conformal mapping programs are written in Fortran. Also included is a graphics program, written in C with X-11 graphics by Mike Stark, for the display of the conformal maps. There are also several demo programs applying the algorithm to problems in elementary fluid flow, extremal length and the hyperbolic geometry. Extensive testing of the geodesic algorithm [MM] and an early version zipper algorithm was done in the 1980’s with Jim Morrow. In particular that experimentation suggested the initial function

φ_0 in the zipper algorithm which maps the complement of a circular arc through z_0 , z_1 , and z_2 onto \mathbb{H} .

Appendix. Jørgensen's Theorem.

Since Jørgensen's theorem is a key component of the proof of the convergence of the geodesic algorithm, we include a short self-contained proof. It says that discs are strictly convex in the hyperbolic geometry of a simply connected domain Ω (unless $\partial\Omega$ is contained in the boundary of the disk).

Theorem A.1 (Jørgensen [J]). *Suppose Ω is a simply connected domain. If Δ is an open disc contained in Ω and if γ is a hyperbolic geodesic in Ω , then $\gamma \cap \Delta$ is connected and if non-empty, it is not tangent to $\partial\Delta$ in Ω .*

Proof. See [P, page 91-93]. Applying a linear fractional transformation, we may suppose that the upper half plane $\mathbb{H} \subset \Omega$. Suppose $x \in \mathbb{R}$ and suppose that f is a conformal map of \mathbb{D} onto Ω such that $f(0) = x$ and $f'(0) > 0$. Then

$$\operatorname{Im}\left(\frac{f'(0)}{f(z)-x} - \left(\frac{1}{z} + z\right)\right)$$

is a bounded harmonic function on \mathbb{D} which is greater than or equal to 0 by the maximum principle. Thus $\operatorname{Im}\frac{f'(0)}{f(z)-x} \geq 0$ on $(-1, 1)$ and hence $\operatorname{Im}f(z) \leq 0$ on the diameter $(-1, 1)$. The condition $f'(0) > 0$ means that the geodesic $f((-1, 1))$ is tangent to \mathbb{R} at x . Thus if γ is a geodesic which intersects \mathbb{H} and contains the point x , then it cannot be tangent to \mathbb{R} at x . Two circles which are orthogonal to \mathbb{R} can meet in \mathbb{H} in at most one point, and hence hyperbolic geodesics in simply connected domains (images of orthogonal circles) meet in at most one point. Thus γ cannot reenter \mathbb{H} after leaving it at x because it is separated from \mathbb{R} by the geodesic $f((-1, 1))$. The Theorem follows. ■

In Section 2, we commented that a constructive proof of the Riemann mapping theorem followed from the proof of Theorem 2.2. The application of Jørgensen's theorem in the proof of Theorem 2.2 is only to domains for which the Riemann map has been explicitly constructed.

Bibliography

- [A] L. Ahlfors, *Lectures on quasiconformal mappings*, Van Nostrand (1966).
- [BT] L. Banjai and L. N. Trefethen, *A multipole method for Schwarz-Christoffel mapping of polygons with thousands of sides*, SIAM J. Sci. Comput. 25 (2003) 1042-1065.
- [GM] J. Garnett and D.E. Marshall, *Harmonic Measure*, Cambridge Univ. Press (2005).
- [H] P. Henrici, *Applied and Computational Complex Analysis*, vol. 3, J. Wiley & Sons(1986).
- [J] Jørgensen, V., *On an inequality for the hyperbolic measure and its applications in the theory of functions*, Math. Scand. 4 (1956), 113-124.
- [K] R. Kühnau, *Numerische Realisierung konformer Abbildungen durch "Interpolation"* Z. Angew. Math. Mech. 63 (1983), 631–637 (in German).
- [L] O. Lehto, *Univalent functions and Teichmüller spaces*, Springer (1986).
- [M] A. R. Marchenko, *Sur la représentation conforme*, C. R. Acad. Sci. USSR vol. 1 (1935), 289–290.
- [MD] D. E. Marshall, *Zipper*, Fortran programs for numerical computation of conformal maps, and C programs for X-11 graphics display of the maps. Sample pictures, Fortran and C code available at URL:
<http://www.math.washington.edu/~marshall/personal.html>
- [MM] D. E. Marshall and J. A. Morrow, *Compositions of Slit Mappings*, unpublished manuscript, 1987.
- [P] Chr. Pommerenke, *Boundary behaviour of conformal maps*, Springer (1992).
- [SS] S. Smale, *On the efficiency of algorithms of analysis*. Bull. Amer. Math. Soc. 13(1985), 87-121.
- [SK] K. Stephenson, *Circle packing: a mathematical tale*, Notices Amer. Math. Soc. 50 (2003), 1376-1388.
- [T] M. Tsuji, *Potential theory in modern function theory*, Chelsea (1975).
- [W] S. Warschawski, *On the degree of variation in conformal mapping of variable regions*, Trans. Amer. Math. Soc. 69 (1950), 335–356.